FUNCTIONALIZATION OF POLY(ETHYLENE OXIDE)-BASED DIBLOCK COPOLYMER VESICLES

A Dissertation

by

KARYM GRACE KINNIBRUGH GARCIA

Submitted to the Office of Graduate Studies of
Texas A&M University
in partial fulfillment of the requirements for the degree of

DOCTOR OF PHILOSOPHY

May 2010

Major Subject: Materials Science and Engineering

FUNCTIONALIZATION OF POLY(ETHYLENE OXIDE)-BASED DIBLOCK COPOLYMER VESICLES

A Dissertation

by

KARYM GRACE KINNIBRUGH GARCIA

Submitted to the Office of Graduate Studies of
Texas A&M University
in partial fulfillment of the requirements for the degree of

DOCTOR OF PHILOSOPHY

Approved by:

Chair of Committee,	Zhengdong Cheng
Committee Members,	Mariah Hahn
	Melissa Grunlan
	Daniel Shantz
Intercollegiate Faculty Chair:	Ibrahim Karaman

May 2010

Major Subject: Materials Science and Engineering

ABSTRACT

Functionalization of Poly(Ethylene Oxide)-based

Diblock Copolymer Vesicles. (May 2010)

Karym Grace Kinnibrugh García, B.S., Pontificia Universidad Católica del Perú

Chair of Advisory Committee: Dr. Zhengdong Cheng

The principal goal of this research is to achieve the chemical labeling and surface modification of block copolymer vesicles (polymersomes) made from amphiphilic diblock copolymer Poly(butadiene-b-ethylene oxide) (PBd_{120}- PEO_{89}, MW 10400 g/mol) with the aim of developing possible drug carrier vehicles for controlled release of molecules triggered by stimuli-responsive environments.

The terminal hydroxyl group of poly(ethylene oxide) (PEO), or poly(ethylene glycol) is converted into its corresponding carboxylic acid by a novel one-pot two-phase oxidation reaction. This regioselective and catalytic reaction assures the preservation of important structural characteristic of the block copolymers. Vesicles formed by a mixture of the carboxylate and unmodified block copolymer exhibit an increment in the critical aggregation concentration (CAC) value while the averaged vesicle size decreases demonstrating that the negative charges in the modified diblock copolymer disrupt the vesicle formation process.

The carboxylated reactive intermediates are subsequently subjected to a covalent coupling reaction in organic solvent to replace the terminal hydroxyl of the PEO block.

The obtained functionalized diblock copolymers are effectively incorporated into the vesicle bilayer. Also, surface density control in polymersomes of fluorescently modified diblock copolymers, synthesized by the amination reaction, is achieved.

To demonstrate the ability of this polymersomes as carrier vehicles, a Noradrenaline functionalized vesicle is placed in closed contact with rat aortic smooth muscle cells (RASMC) using the micropipette aspiration technique. A distinctive increase in fluorescent intensity of cells is observed. It indicates that the drug molecule has been transported by the polymersome and internalized by the cell. In addition, diblock copolymers containing a disulfide moiety and a fluorophore are synthesized and studied through fluorescent microscopy. Vesicles are formed with this polymer and a decrease in fluorescent intensity is observed in the vesicle's bilayer after its exposure to a reductive environment. These results indicate that fluorophore molecules are successfully released into solution.

DEDICATION

TO MY PARENTS, AUNT, AND UNCLE

I thank you for all your love, moral support and encouragement. To my mother, for giving me the strength I needed, and to my father, for inspiring me.

ACKNOWLEDGEMENTS

I would like to express my gratitude to my committee chair, Dr. Zhengdong Cheng, for assuming the role of my research advisor and willingly helped me through the final stage of my PhD studies with valuable guidance, input and encouragement.

I want to extend my deep gratitude to my former research advisor, Dr. James Silas, for teaching me how to think as a scientist, elaborate an appropriate research plan and conduct relevant studies. Thank you very much for the confidence you gave me from the beginning and, your constant motivation. Thank you for being a good mentor and a better human being.

I also want to thank Professor Mariah Hahn for the direction provided during cell studies and for making them possible by the generous sharing of her laboratory facilities. I thank Professor Melissa Grunlan for the use of the FT-IR equipment for organic compounds identification. I acknowledge the support provided by TEES, TAMU, NSF REU program (grant 0552655), and the Materials Characterization Facility (MCF) of TAMU for the use of the confocal microscope and the spectrofluorometer.

Thanks also to my friends and colleagues who helped me in many ways to make this work possible: Ranjini Murthy, Jesús López-Domínguez, Jeffery Gaspard, Clemente Contreras, Ya-Weng Chang, and Dany Muñoz-Pinto.

Finally, thanks to my beloved friends and family, particularly to my mother, my dearest aunt, and uncle for their constant support, encouragement, patience, and unconditional love.

I have fought the good fight, I have finished the race, I have kept the faith.

2 Timothy 4:7

TABLE OF CONTENTS

CHAPTER Page

CHAPTER Page

LIST OF FIGURES

FIGURE Page

FIGURE Page

FIGURE Page

FIGURE Page

FIGURE Page

LIST OF TABLES

CHAPTER I

INTRODUCTION

1.1 Overview

Over the years, many traditional drug therapies have failed to perform efficiently and in several cases the side effects of the administered drug caused more distress to the patience. In order to reduce the possibility of under and overdosing, among other possible life-threatening situations, polymeric vesicles arise as promising controlled-release drug delivery vehicles (see Figure 1.1).

Ideally, polymeric vesicles will help to keep constant the required drug level in the body, fewer doses will be required, effective retention of different encapsulates will be accomplish and specific triggered and controlled release of contents will be achieved. However, other design considerations are still complicated to incorporate into the vesicle's architecture such as biocompatibility, biodegradability over suitable periods of time, extended blood circulation, and non-toxic byproducts. In summary, this attractive devices need to be functionalized and tailored for specific uses and subjects. Thus, functionalization of polymeric vesicles is still of significant interest for the scientific community.

This dissertation follows the style of Biomaterials.

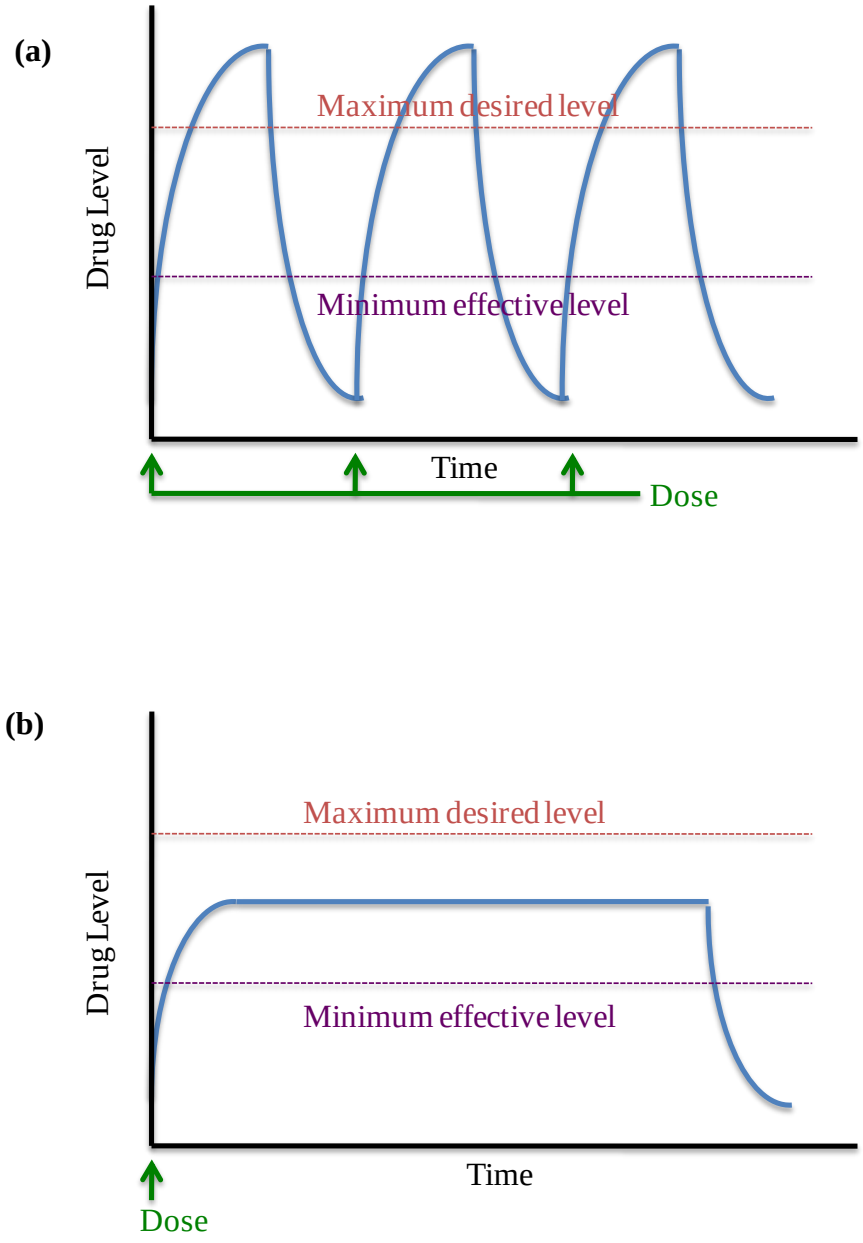

Figure 1.1 Schematic representation of drug levels in blood stream in (a) traditional drug administration and dosage and (b) controlled delivery dosage. (a) Drug dosing can fall below or above the required treatment level in between the multiple doses required which can produce life threatening situations for the patient. (b) Using controlled drug delivery, a single dose can keep steady levels of drug in blood.

1.2 Phospholipids and Cell Membrane Composition

During the last century, it has been realized that all living matter is composed of cells, that cells are organized into compartments, and that cell walls are composed of bilayers of lipid molecules [1-4]. Natural phospholipid molecules found in cell membranes are amphiphili*c* molecules of molecular weight less than 1 kilodalton with one water-soluble end and one hydrophobic end. The water-soluble end is usually charged while the hydrophobic end is usually one or more hydrocarbon chains. The lipids found in cell membranes are mostly molecules with two hydrocarbon chains of about 10 carbons.

When phospholipids are suspended in water they can form a variety of structures but in all cases the hydrophilic phosphate region interacts with water and the hydrophobic fatty acid regions are excluded to form hydrophobic interactions. This self-directed assemble is possible because the charged ends of the phospholipids have lower free energy when in contact with the surrounding water while the opposite is true for the hydrocarbon tails. The latest ones eliminate most of their contact with water if they organize themselves into bilayers of about 5 nm and, when closed into “bubble type structures”, bilayers provide a barrier between inside and outside defining closed compartments. Large bubbles of this type with many microns in diameter are called vesicles or liposomes [5-14].

1.3 Lipid Vesicles and Biological Membranes

The discovery of liposomes is credited to A.D. Bangham while performing research on blood cloths in 1961 [15]. Bangham first observed that in aqueous solutions, phospholipids spheres were formed and he cited: *"Liposomes are the smallest artificial vesicles of spherical shape that can be produced from natural nontoxic phospholipids and cholesterol. Liposomes are microscopic, fluid-filled pouches whose walls are made of layers of phospholipids identical to the phospholipids that make up cell membranes"*. Since 1811, research reports described the binding of phosphorous molecules to fatty acid chains, presence of lipid-like substances in biological samples and, growth of cylindrical structures from lipids extracted from brain tissue. Still, it was not until the a hundred years later when the introduction of the electron microscope helped with the characterization of close packed lipid structures [16-18].

However, it was not until the 1970's that the potential use of lipid vesicles as packaging agents and drug delivery systems was recognized [19-22]. During 1980's, distribution of injected liposomes formulations by the circulatory system was the main focus of this research area [23-31], and throughout 1990's, gene therapy and gene diagnosis applications of liposomes prevail [30, 32]. On the other hand, the relative success of lipid vesicles as drug delivery vehicles contrasts with the difficult control of lipid properties when long-standing use is required such as, lipid stability in biological fluids, long-term storage and cell targeting. Lipid vesicles play an important role in cell function as compartmentalizing structures, nutrient transport facilitators, DNA protective agents, and they can entrap dissolved substances as well as hydrophilic and hydrophobic

compounds inside the membrane cores. Due to the dynamic and soft character of lipids [33-35], when more than $100x10^3$ amphiphiles aggregate into a membrane, properties such encapsulant retention ability, membrane stability and degradation become difficult to control [36-38]. For that reason, a polymer mimic of lipid ones emerged as an alternative since its structure resembles that of a living cell. Polymer vesicles will also help to take a closer look to the principles of natural design of biological membranes and membrane mediated events [39-42].

1.4 Polymersomes: A Polymer Mimic of Lipid Vesicles

Small amphiphilic molecules such as lipids have inspired the use of synthetic analogs of higher molecular weight defined as super amphiphiles, category that includes linear diblock copolymers. In the last decades, an increase interest in the use of artificial block copolymers to produce cell-like vesicles, also called polymersomes, was reported because of their unique properties. These artificial bilayer structures can be formed by self-assembly of synthetic diblock copolymers and the produced synthetic vesicles exhibit superior material characteristics making them tougher than lipid vesicles [43-44].

Block copolymers have similar design as phospholipids and these are formed by covalent linking of two (diblock copolymers) or more polymer segments that usually are much larger than the lipid ones [45-47]. In the presence of a solvent, they will self assemble into different structure types determined by the hydrophilic-hydrophobic diblock ratio: membranes, micelles, rod-like or spherical vesicles (see Figure 1.2).

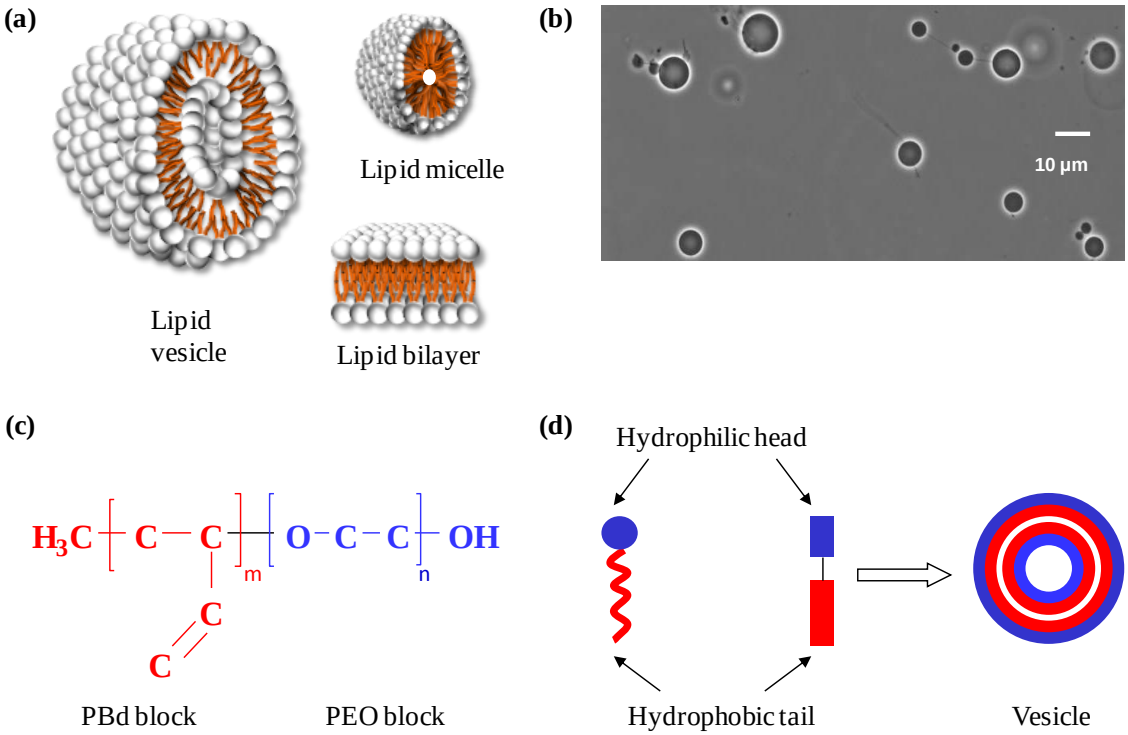

Figure 1.2 Schematic representation of natural phospholipids (a), microscopy image of $PBd_{120}PEO_{89}$ diblock copolymer vesicles (b), chemical structure of PBd_mPEO_n diblock copolymer (c), and self-assembly of phospholipids and diblock copolymers into vesicle structures (d). Natural phospholipids and synthetic diblock copolymers consist of hydrophobic and hydrophilic segments; both will self-assemble in aqueous solution to form vesicles.

The mechanical properties of polymersomes have been studied by micropipette aspiration technique. Their elastic, determined by measurement of membrane tension (τ, mN/M) versus area expansion ($\alpha = \Delta A/A_0$), behavior was proved to be superior to that of lipid vesicles (see Figure 1.3). Its increased chain length provides toughness (determined by membrane aspiration to the point of rupture) and reduces membrane permeability (considerable reduced transport rate) which enable polymersomes as new artificial and resistant delivery vehicles [48-50]. The chemistry of these novel structures can be

manipulated by controlling the diblock molecular weight, block ratio, and architecture of the block copolymer used [51-53].

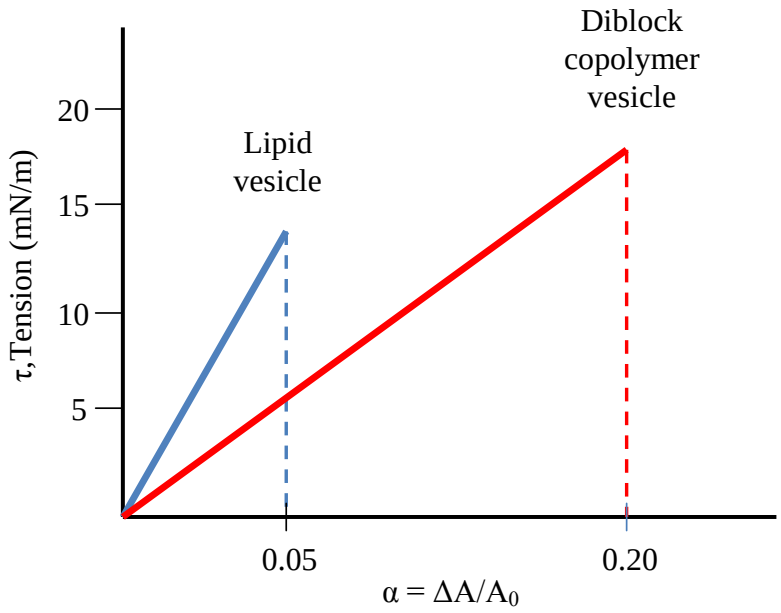

Figure 1.3 Schematic representation of increased mechanical resistance of diblock copolymer vesicles compared to lipid vesicles. Polymer vesicles can stand greater mechanical deformations (~0.20 %) before rupture than lipid vesicles (~0.05%).

Formation of Polymersomes

Polymersomes can be formed from diblock copolymers where the hydrophobic region has a high glass transition temperature (Tg) like polystyrene (PS) and the hydrophilic part is ionic (like poly-(acrylic acid), PAA) or when the overall molecular weight of the diblock copolymer is higher than the one for lipids (much greater than 10 kD) [54]. The general procedure of polymersome preparation includes the dissolution of the diblock copolymer in an appropriate solvent for both blocks (dioxane for PS-PAA case), a drying step that allow a thin polymer film formation (micrometers thick), and

addition of water to precipitate vesicles. Water promotes aggregation of PS and formation and increase of interfacial tension. This very last step, the rehydration of the polymer film, will introduce the key to the utilization of polymersomes as drug delivery vehicles (see Figure 1.4). Any water based solution containing drugs, proteins or any kind of molecule will be encapsulated inside the polymersome during the rehydrating step. Retention of captured molecules, such as dextrans, sucrose or physiological saline, have been proved to remain stable over periods of several months inside of ~100 nm polymersomes and ~10 μm giant vesicles [55-56].

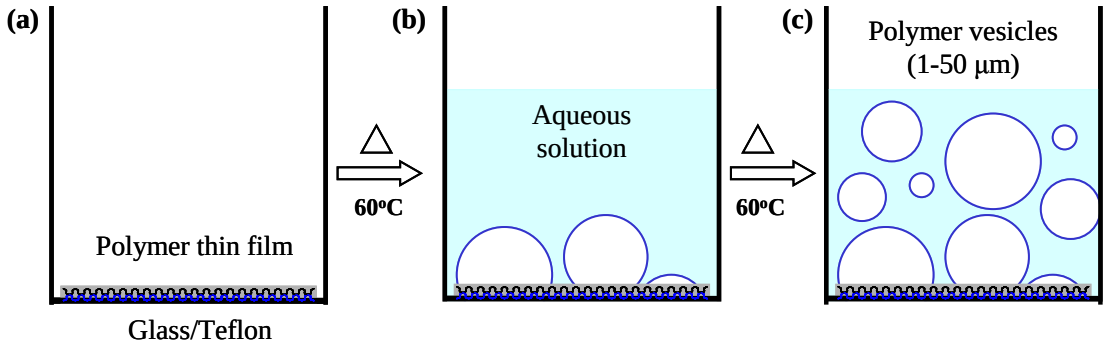

Figure 1.4 Formation of diblock copolymer vesicles in aqueous solution at 60ºC. Polymeric vesicles will spontaneously self-assemble in order to minimize the system's surface tension energy. (a) A thin polymer film was formed over a glass or Teflon® surface after a drying process. (b) An aqueous solution was added and heated overnight at 60ºC. (c) Diblock copolymer vesicles suspended in solution.

Formation of polymersomes in aqueous solvents can also be accomplished. Extensive research has been done using polyethylene-b-polybutadiene (PEO_m-PBd_n), as well as it hydrogenated homolog polyethylene-b-polyethylethylene (PEO_m–PEE_n), to form vesicles under different aqueous environments. Doxorubicin, an anti-neoplastic

agent, was encapsulated during rehydration by the polymer vesicle with liposomes similar efficiency increasing the potential of using polymersomes as artificial controlled-release systems. Other approaches on the use of polymersomes as synthetic drug delivery devices are reviewed in the following sections [57].

Applications of Polymersomes

Triblock copolymers can also form polymersomes with some useful differences with respect to membrane properties. Pluronic®, a large triblock copolymer (PEO_5-PPO_{68}-PEO_5) composed of a large poly-(propyleneoxide) (PPO) midblock, forms small vesicles in water media with thin membranes of 3-5 nm and a short life of hours only, which will suggest that this midblock weaken the polymeric structure. Another example of vesicle forming triblock is composed of a hydrophobic midblock of poly-(dimethylsiloxane) (PDMS) and two polar blocks of poly-(2-methyloxazoline) (PMOXA) with crosslinkable methacrylate ending groups.

Block copolymers with a bioinert block and a hydrophilic block that can undergo hydrolytic degradation have been extensively studied as a possibility for in vivo biodegradable drug delivery polymersomes [58-60]. However, a new amphiphilic diblock copolymer system of PEO and poly-(caprolactone) (PCL), both of them used in FDA–approved medical devices, promise to form completely bioresorbable vesicles with no toxic byproducts as a result of its degradation. Again, PEO [57] was chosen because of its biocompatibility and also because it gives to the vesicles longer blood circulation times [61-62]. PCL will form the hydrophobic membrane portion of the vesicle. It

degrades safely and completely by hydrolysis of its ester bond under physiological conditions which makes itself a suitable implantable biomaterial for drug delivery vehicles. Among the advantages of PCL are: elevated permeability to small molecules, pH of the media is preserved after degradation, it mixes well with other polymers, and its slow degradation (by erosion mechanism) makes it appropriate for long-term drug delivery. Vesicles of 10-20 μm diameter, ideal size for in vivo applications, were formed and size was controlled either by sonication or freeze/thaw technique followed by extrusion above 65°C. A wide range of PEO-b-PCL block copolymers with different molecular weights were studied being only PEO(2K)–b–PCL(12K) the one to give a good yield of vesicle formation via spontaneous self assembly [63].

Doxorubicin was dissolved in the aqueous solution of dehydration of PEO(2K)-b- PCL(12K) polymersomes in order to elucidate the mechanism by which a drug is released. Doxorubicin in situ released under physiological conditions such as pH 5.5 and 7.4, and 37°C was monitored fluorometrically for 14 days. At both pH conditions at 37°C, an instantaneous burst release was registered (20 % of vesicle filling, from 0 to 8 hours), proceeded by controlled release. The drug releasing process can be cataloged into two different steps: First the drug was released mainly by its diffusion through PCL membrane and although hydrolytic degradation of the PCL membrane is observed, it is not of much importance. A second drug release occurred due to significant hydrolytic PCL membrane degradation. At ph 7.4 the first and second types of drug release were observed while at pH 5.4 only the second type predominates. Hence, in vivo drug release of PEO(2K)-b-PCL(12K) is both dependent on PCL matrix erosion and drug's specific

permeability through the vesicle membrane. In comparison with polymersomes that undergoes hydrolytic degradation over a small period of time (hours), PEO(2K)-b-PCL(12K) exhibits slower rates of drug releasing (days).

Other functionalized self-assembly polymersomes includes copolymers of PEO – PPS (poly-(propylenesulfide)) where the PPS groups are susceptible to undergo oxidative degradation. PEO-PLA (poly-(lactide)) kilodalton-size block copolymers form micelles that can be biodegraded by hydrolytic scission raising the possibility of its use for controlled drug release. Therefore, biodegradable vesicles for controlled drug release of its contents are feasible.

Also, PEO-PEE polymersomes were injected into blood stream of rats and it was shown that they behave as liposomes. They circulated for 15-20 hours before being captured by phagocytes of liver. In a parallel test tube study in cell–free blood plasma, it was shown that plasma proteins slowly accumulate over the polymersome membrane followed by cell attachment. This effective delay was provided by the brush surface of the PEO which acts like a biomembrane. These results emphasize polymersomes as biomedical a promise.

Thus, synthetic polymer vesicles can also mimic many biological membrane processes, such as protein integration, fusion and DNA encapsulation [64]. Polymer versatility regarding molecular weight, polydispersity, reactivity, and synthetic diversity provide a broad spectrum of approaches to vesicle design for drug delivery. However, actual polymersomes still exhibit a structural stability that relays on several intrinsic and environmental parameters which commonly ended up affecting its efficacy as drug

delivery vehicles [65]. The degradation periods are still not long enough for controlled long-term in vivo drug release and small periods of circulation time are considered as important drawbacks of this polymersomes design. Also, the absorption of macromolecular drugs such as peptides and proteins to polymersome walls and protein configuration changes caused by polymer interactions are other disadvantages of polymersomes still to be solved.

General considerations for future polymersome designs for *in vivo* controlled drug delivery will include the biocompatibility and biodegradability of the hydrophobic component, extended degradable periods and extended circulation times in blood stream, and non-toxic degradation products that can be metabolized and excreted by the human body [66-67]. Not only exerted control over chain length of the block copolymers and ratio of amphiphile components are important for polymersome design but also, the molecular weight and polymer structure (linear or branched) should be controlled to explore the possibility of size and surface modifications.

1.5 Dissertation Outline

Chapter II: Oxidation of Primary Alcohol end Group of $PBd_{120}PEO_{89}$ Diblock Copolymer

- The free hydroxyl terminal end group of the block copolymer Poly(butadiene-b-ethylene oxide) ($PEO_{89}PBd_{120}$, MW 10400 g/mol) is oxidized to its corresponding carboxylic acid (carboxylate $PBd_{120}PEO_{89}$) through a selective two phase oxidation reaction while other oxidizable groups remain unaffected.

- The CAC values of vesicle solutions containing a mixture of carboxylate $PBd_{120}PEO_{89}$ and unmodified $PBd_{120}PEO_{89}$ increase when the percentage of carboxylate $PBd_{120}PEO_{89}$ is increased, while the average vesicle size decreases. No vesicle formation is observed at concentrations higher than 80% are reached.

Chapter III: Covalent Coupling of Primary Amine to Carboxylate PBd_{120}-PEO_{89} Diblock Copolymer

- Three different primary amines were covalently attached to the previously synthesized carboxylate block copolymer through a modified amination reaction performed in organic phase.
- Polymersomes containing 90% of the unmodified block copolymer and 10% of one of the modified block copolymers ($PBd_{120}PEO_{89}$-6AF, $PBd_{120}PEO_{89}$-COU, and $PBd_{120}PEO_{89}$-NA) were prepared.
- Two types of modified diblock copolymers ($PBd_{120}PEO_{89}$-6AF, $PBd_{120}PEO_{89}$-COU) were also properly integrated into the same vesicle and, surface density control of the two fluorophores was achieved and confirmed through fluorescence microscopy.

Chapter IV: Cell Response to Hormone Functionalized PBd_{120}-PEO_{89} Diblock Copolymer

- Noradrenaline molecules were transported from the surface of functionalized vesicles to smooth muscle cell surfaces.
- A cell response was produced (increase in fluorescent intensity) after noradrenaline molecules bound to surface cell receptors.

Chapter V: Reduction-Responsive Functionalized $PBd_{120}PEO_{89}$ Diblock Copolymer Vesicles

- The functionalized reductive-responsive diblock copolymer $PBd_{120}PEO_{89}$-cystamine-5-tetramethylrhodamine (5-TAMRA) was synthesized using a one-pot two-step reaction and was incorporated into polymersomes in a 10% amount.
- The reductive character of the diblock was given by the presence of a disulfide linkage between the PEO block and the 5-TAMRA fluorophore molecule.
- The diblock copolymer disulfide bonds were selectively reduced when exposed to tris(2-carboxyethyl)phosphine hydrochloride (TCEP) and the fluorophore 5-TAMRA was released into solution causing a decrease in the vesicle's bilayer fluorescent intensity of 44 %.

Chapter VI: Conclusions and Future Directions

In this dissertation research, the modification of polymersomes' surface by the introduction a functionalized diblock copolymer into the vesicle's bilayer was achieved.

Three functionalized PEO-PBd diblock copolymers were created using novel and simple synthetic pathways; they were effectively incorporated into the vesicle structure and characterized by microscopy techniques. Vesicle surface properties were studied and the polymersome's ability to deliver a drug molecule was tested using *in vitro* cell cultures. Hence, these studies contribute to the better understanding of functionalized diblock copolymer vesicles and its application as drug delivery devices.

For future studies, biodegradable diblock copolymers may be used instead and apply to it the synthesis explored during this research. Investigate the cell internalization process and degradation time to elucidate the cell's response mechanism. Also, stimuli-responsive functionalized polymersomes vulnerable to reducible atmospheres might be evaluated in contact with smooth muscle cell cultures to establish the reductive strength of the cytoplasmic environment over the disulfide moieties employed.

A reductive destabilization mechanism involving a phase transition from vesicle to micelle of a PEO-PBd diblock copolymer linked to a second PEO block by a cystamine molecule can be synthesized and polymersomes containing this PEO-PBd-cystamine-PEO amphiphillic polymer might be formed and studied.

CHAPTER II

OXIDATION OF PRIMARY ALCOHOL END GROUP OF $PBd_{120}PEO_{89}$ DIBLOCK COPOLYMER

2.1 Overview

The carboxylate derivative of the diblock copolymer polybutadiene-b-poly(ethylene oxide) ($PBd_{120}PEO_{89}$, MW 10400 g/mol), **(2)**, was prepared by a one pot two-phase oxidation reaction. This mild and regioselective catalytic reaction effectively oxidize only the primary alcohol end group of the polyethylene oxide block leaving unaffected any other susceptible groups, such as ether linkage of polyethylene oxide or C=C double bonds of the polybutadiene block. Vesicles containing the carboxylate derivatives were formed and the critical aggregation concentration (CAC) values of the vesicle solutions were measured.

2.2 Introduction

Due to PEO unique properties and applications the functionalization of PEO has been the focus of many researches [68-71]. However, the conversion of its free terminal hydroxyl group into an aldehyde or carboxylic acid has not been completely successful and many reaction procedures have been proposed. For example, the use of pyridine chlorochromate or dichlorochromate, suggested by Corey [72], affects other oxidizable groups of the polymer chain, such as carbon-carbon double bonds and ether linkages,

because a strong reaction condition was used and, hence only limited yields were obtained. A more selective and mild reaction was proposed by Kornblum [73] to use dimethyl sulfoxide as the oxidation reagent. Also, Mosbach [74-76] suggested the use of organic sulfonyl chlorides (tosyl and tresyl chloride), which formed good leaving groups that facilitates the formation of the respective carbonyl derivative. Nevertheless, the reaction conditions were still not easy to achieve and it was still not possible to discriminate between the oxidation of primary and secondary alcohol groups when present in the same molecule. Later on, Anelli [77-78] and coworkers suggested the use of 4-methoxy-2,2,6,6-tetramethyl-piperidine-1-oxyl (TEMPO), a nitroxyl radical catalyst, to regioselectively oxidize primary alcohol groups as a mild and environmentally friendly catalytic method.

Herein, we propose a strategic synthesis to convert the primary hydroxyl end group of $PBd_{120}PEO_{89}$ diblock copolymer into its corresponding carboxylic acid using a modified version of the Anelli's protocol. This oxidation reaction was performed using a two phase (dichloromethane and water) system where TEMPO is continuously regenerated in the aqueous phase; in conjunction with a sodium hypochlorite (NaOCl) solution to regioselectively oxidize the free primary alcohol group of the block copolymer leaving intact any other groups.

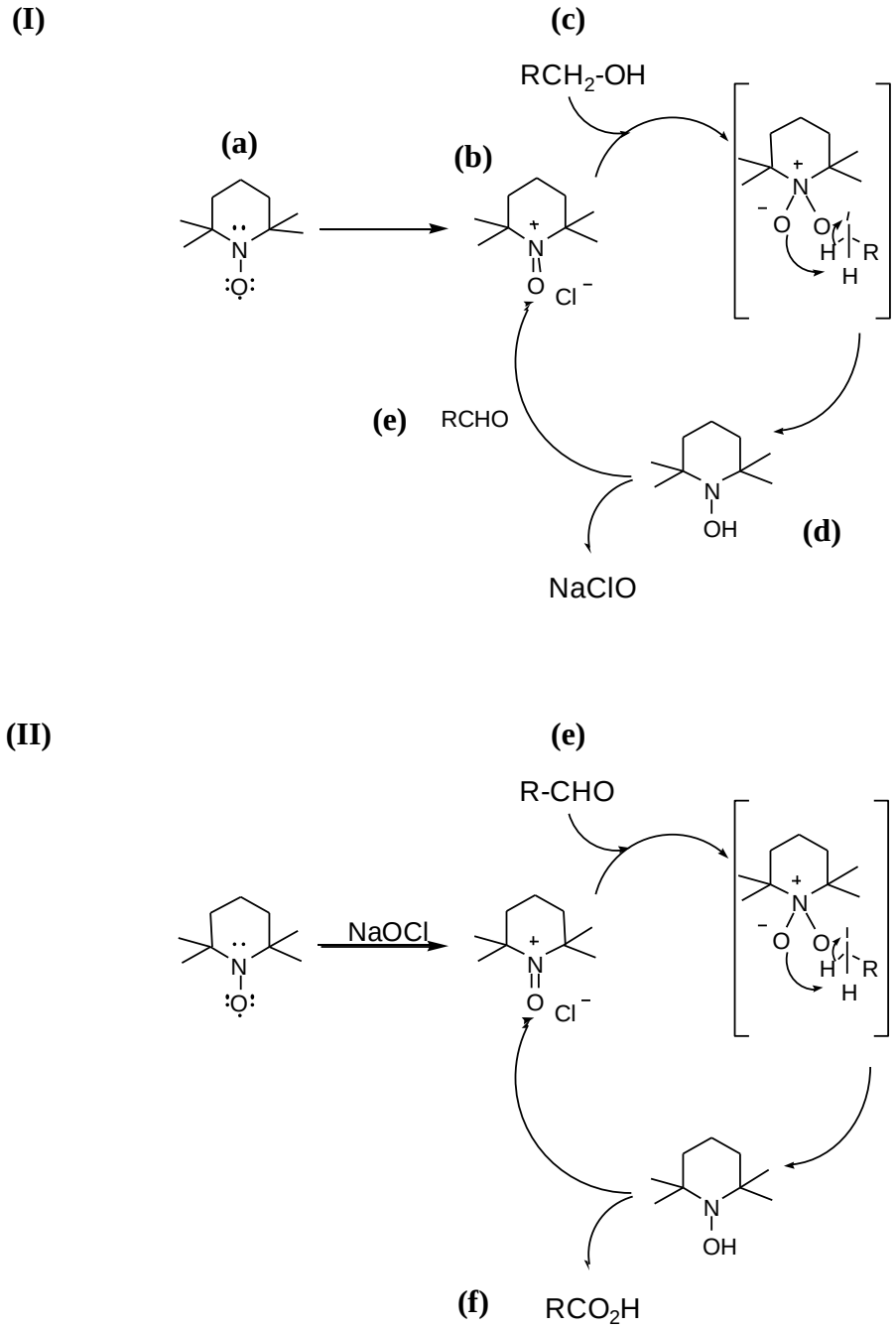

Figure 2.1 Catalytic cycle of TEMPO during oxidation reaction of a primary alcohol (c) to the respective carboxylic acid (f). Figure 2.1.I shows that TEMPO (a) was first oxidized by NaClO to its respective N-oxoammonium salt (b); this oxidized the primary alcohol end group of the PEO block (c) to its aldehyde (d) in the organic phase while (b) is also regenerated. Figure 2.1.II shows that (d) returned to the catalytic cycle (aqueous phase) to further oxidize the aldehyde in its respective carboxylic acid (f).

Figue 2.1 shows the TEMPO catalytic cycle where it (a) was first oxidized by NaOCl to the respective N-oxoammonium salt (b), the primary alcohol end group of the PEO block (c) was oxidized to aldehyde (e) by the N-oxoammonium salt, and a molecule of the hydroxylamine (d) was produced. The aldehyde (e) was then oxidized by NaClO to carboxylic acid (f) and a molecule of NaOCl was regenerated [71, 79-83].

This formulation uses the oxidation agent NaOCl only, no addition of potassium bromide or quaternary ammonium salt (suggested by Anelli's protocol) was required, and it was performed at room temperature for 3-5 minutes. This constitutes an environmentally friendly catalytic method executed via mild conditions and less harmful chemicals.

Figure 2.2 sketches the chemical structures of the diblock copolymer polybutadiene-b-poly(ethylene oxide) ($PBd_{120}PEO_{89}$) used as a starting material **(1)** and its oxidized derivative where the free hydroxyl end group is converted into the corresponding carboxylic acid, carboxylate $PBd_{120}PEO_{89}$ diblock copolymer **(2)**.

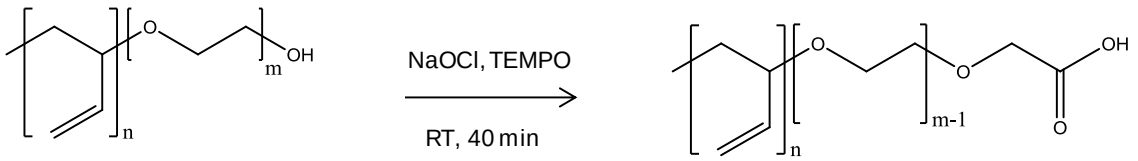

(1) **(2)**

Figure 2.2 Oxidation reaction of primary alcohol end group of polybutadiene-b-poly(ethylene oxide) ($PBd_{120}PEO_{89}$) diblock copolymer. A carboxylate $PBd_{120}PEO_{89}$ diblock (2) is produced.

Once the carboxylate block copolymer is obtained, the critical aggregation concentration (CAC) [84] of vesicles formed by a blend of varying ratios of unmodified $PBd_{120}PEO_{89}$ and carboxylate $PBd_{120}PEO_{89}$ will be measured in order confirm the presence of the carboxylate derivative and to physically characterize the new product.

2.3 Materials

Poly(butadiene-b-ethylene oxide) (PBd_{120}-PEO_{89}, MW 10400 g/mol) block copolymer and sucrose (ACS reagent) ($C_{12}H_{22}O_{11}$, MW 342.3 g/mol) were purchased from Polymer Source Inc. (Canada) and Fisher Scientific (Pittsburgh, PA), respectively. Dichloromethane (anhydrous, 99.9%) (CH_2Cl_2, MW 84.93 g/mol), chloroform (99.8+% for analysis ACS, stabilized with ethanol) ($CHCl_3$, MW 119.38 g/mol) and methanol (99.8+% for analysis ACS) (MeOH, MW 32.04 g/mol) were purchased from Acros Organics (Morris Plains, NJ). 4-methoxy-2,2,6,6-tetramethyl piperidine-1-oxyl (TEMPO, 156.25 MW g/mol); sodium hypochlorite (NaOCl, MW 74.44 g/mol); sodium bicarbonate ($NaHCO_3$, MW 84.01 g/mol), potassium chloride (KCl, MW 74.55 g/mol) and sodium hydroxide (NaOH, MW 40.00 g/mol) were purchased from Sigma-Aldrich (St. Louis, MO). Regenerated cellulose dialysis tubing kit (MWCO 8000 g/mol) was purchased from Spectra/Por®Biotech.

2.4 Experimental Methods

Diblock Copolymer Characterization

IR Spectroscopy. IR spectra of neat liquids were performed using a Bruker FT-IR TENSOR™ spectrometer (Billerica, MA) equipped with OPUS™ measurement software. Potassium bromide salt plates (McCarthy Scientific Co., Fallbrook, CA) and CH_2Cl_2, or $CHCl_3$, were used to evaluate the polymer samples.

Vesicle Solution Characterization

Conductivity Measurements. A series of 11 vesicle solutions were prepared by mixing PEO_{89}-PBd_{120} and carboxylate PEO_{89}-PBd_{120} in ratios from 0:1 to 1:0 respectively. The conductivities of each original sample and its correspondent subsequent dilutions (12-15 dilutions) were recorded using a Mettler Toledo pH meter (S20 SevenEasy™, Columbus, OH), with a calibrated cell constant, and a Mettler Toledo pH microelectrode (InLab® 423). Ultra pure water (18.2 MΩ-cm) was used to prepare the vesicle solutions and to dilute them. Potential measurements (mV) for each sample, expressed as conductivity values (μS/cm), were plotted against the respective polymer concentration (μM) in order to find the critical aggregation concentration (CAC) value of the sample.

Microscope Imaging. Vesicle solutions were imaged using a temporary closed sample chamber constructed using a microscope slide, microscope glass cover, a silicone rubber and vacuum grease. In order to provide adequate contrast for imaging, a 310 mOsm/kg NaCl solution was placed into the temporary chamber followed by a smaller

amount of the vesicle solution under study (300 mOsm/kg). Phase contrast images of polymersomes were taken by a Carl Zeiss Axiovert 200M inverted microscope with 100 W HBO Mercury vapor lamp coupled to a Zeiss AxioCam MRm camera and a 20X objective (numerical aperture of 0.5).

2.5 Synthesis of Carboxylate $PBd_{120}PEO_{89}$

A 20 mL reaction flask was charged with 1 mL of a CH_2Cl_2 solution of $PBd_{120}PEO_{89}$ diblock copolymer (MW 10400 g/mol), 1.38 mL of a 0.016M CH_2Cl_2 solution of TEMPO and 5.72 mL of a 0.35 M aqueous sodium hypochlorite (NaOCl) solution buffered with $NaHCO_3$ at pH 8.6. The reaction mixture was magnetically stirred at 900 rpm using a Teflon-covered stir bar. Doses of 1 mL of 0.016 M CH_2Cl_2 solution of 4-methoxy-2,2,6,6-tetramethyl piperidine-1-oxyl (TEMPO) were added every 3-5 min at room temperature. Once the reaction was completed, pH was adjusted at $\geq$ 11 with aqueous 3N NaOH in order to breakdown the formed emulsion. The organic phase was separated from the mixture and dried out in a vacuum oven. After the cleaning procedure, the final product was dried out in a vacuum oven and redisolved in CH_2Cl_2. An aliquot of the reaction solution was evaporated on a NaCl plate and the IR spectrum was obtained.

Synthesis of (2)

PBd_{120}-PEO_{89} (40.0 mg, 3.85×10^{-3} mmol), TEMPO (13.22 mg, 8.46×10^{-2} mmol), and NaOCl (97.46 mg, 1.31 mmol) were reacted in dichloromethane/water as described

above. In this manner, product **1** (30.4 mg, 76% yield) was obtained. IR (ν): 1725 (C=O) cm^{-1}.

Functionalized Diblock Copolymer Cleaning Procedure

The desired product, contained in the organic phase, was redisolved in 2 mL of a 1:1 MeOH:$CHCl_3$ solution and cleaned using regenerated cellulose dialysis tubing (MWCO 8000 g/mol). The sample was dialyzed for 2 hours at room temperature against 600 mL (300 times the volume of the sample) of 1:1 MeOH:$CHCl_3$ solution, the dialysis buffer was changed and the sample dialyzed for another 2 hours. Finally, the dialysis buffer was changed for the second time and the sample dialyzed overnight.

2.6 Vesicle Solution Preparation

A polymer film containing 100 μg of the desired block copolymer or block copolymer mixture was formed by evaporation (8 hours) at the bottom of a 5 mL glass scintillation vial. Polymersomes were formed by rehydration of this polymer film during 24 hours at 60ºC with 2 mL of the desired solution: ultrapure (for conductivity measurements only) water or 300 mOsm/kg sucrose solution (osmometer model 3320, Advanced Instruments, Inc., Norwood, MA). In the case of vesicles formed with a mixture of block copolymers, X% w/w of carboxylate PBd_{120}-PEO_{89} block copolymer was ideally mixed with Y% w/w of unmodified PBd_{120}-PEO_{89} block copolymer before the polymer film formation step. Vesicle solutions of the mixture compositions shown in Table 2.1 were formed.

Table 2.1 Vesicle solution compositions of unmodified $PBd_{120}PEO_{89}$ and carboxylate PBd_{120}-PEO_{89} mixtures used for CAC measurements.

Vesicle Solution*	% w/w unmodified $PBd_{120}PEO_{89}$	% w/w carboxylate $PBd_{120}PEO_{89}$
1	100	0
2	90	10
3	80	20
4	70	30
5	60	40
6	50	50
7	40	60
8	30	70
9	20	80
10	10	90
11	0	100

*The final block copolymer concentration in a 2 mL vesicle solution is 4.8 μM.

Measurement of CAC of Vesicle Solutions

CAC values can be determined by measuring the surface tension, conductivity, surfactant ion exchange, or ultraviolet absorbance of a copolymer solution due to a drastic change in these physical properties at the CAC. We determined the CAC's of the mixtures by conductivity measurements to locate the concentration where the conductivity rapidly plateaus.

The solution voltage was measured by a pH meter and Ohm's Law ($V = IR$) was used to convert voltage into resistance and afterward, resistance (R) into conductance (G). Conductivity differs from conductance by a proportional factor which is specific to the apparatus. This factor was determined by measuring experimental conductance values of KCl solutions that were plotted against literature conductivity values [85].

Conductivity was plotted against diblock copolymer concentration values. As the concentration increased, the conductivity values increased rapidly and, when the critical aggregation concentration (CAC) was reached, the conductivity plateaus. This point was identified by the intersection of the best linear fit of the two data regions on the conductivity-concentration plot. The experimental CAC values obtained were plotted against carboxylate $PBd_{120}PEO_{89}$ concentration and, CAC values were also modeled by iterating equation 12 and substituting the resulting x_1 values into equation 6 [43, 86-88].

2.7 Results and Discussion

Synthesis of Carboxylate $PBd_{120}PEO_{89}$

The two-phase regioselective oxidation reaction successfully produced and a 76% yield was obtained. A distinctive C=O transmittance band was observed at 1725 cm^{-1} in the respective IR spectra contrasting with the starting material one.

Verification of Composition of Carboxylate $PBd_{120}PEO_{89}$

One of the main concerns regarding this oxidation procedure is to preserve other groups that is present in the polymer chain, such as the C=C and C-H bonds of the butadiene block and the C-O bond of the polyethylene oxide block, since they are also susceptible to oxidation. Figure 2.3 shows the overlay IR spectra of the unmodified $PBd_{120}PEO_{89}$ and the carboxylate $PBd_{120}PEO_{89}$. The presence of a peak at around 1725 cm^{-1} in the carboxylate $PBd_{120}PEO_{89}$ IR spectra corresponding to a carbonyl stretch demonstrates that the oxidation of the free terminal hydroxyl group of $PBd_{120}PEO_{89}$, first

to an aldehyde and then to a carboxylic acid. The original characteristic peaks are preserved (C-H, C=C and C-O stretches) meaning that other groups present in the original diblock copolymer were not oxidized.

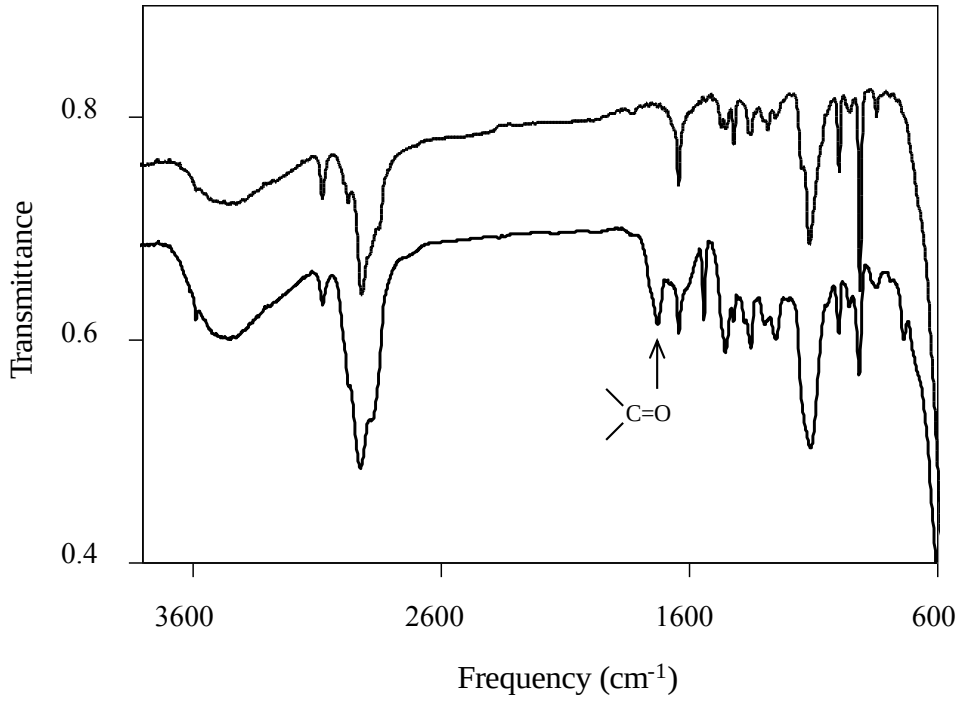

Figure 2.3 Comparison between the IR spectra of the unmodified $PBd_{120}PEO_{89}$ (top) and the carboxylate $PBd_{120}PEO_{89}$ (bottom). The carbonyl stretch (1725 cm^{-1}) demonstrates that block copolymer was effectively oxidized to its carboxylic acid.

CAC Measurements and Microscope Imaging

Figure 2.4 shows the CAC values corresponding to $PBd_{120}PEO_{89}$ vesicle solutions formed with 0 to 100 percent of carboxylate $PBd_{120}PEO_{89}$. As the carboxylate $PBd_{120}PEO_{89}$ amount is increased, the CAC values increases while the average vesicle size decreases.

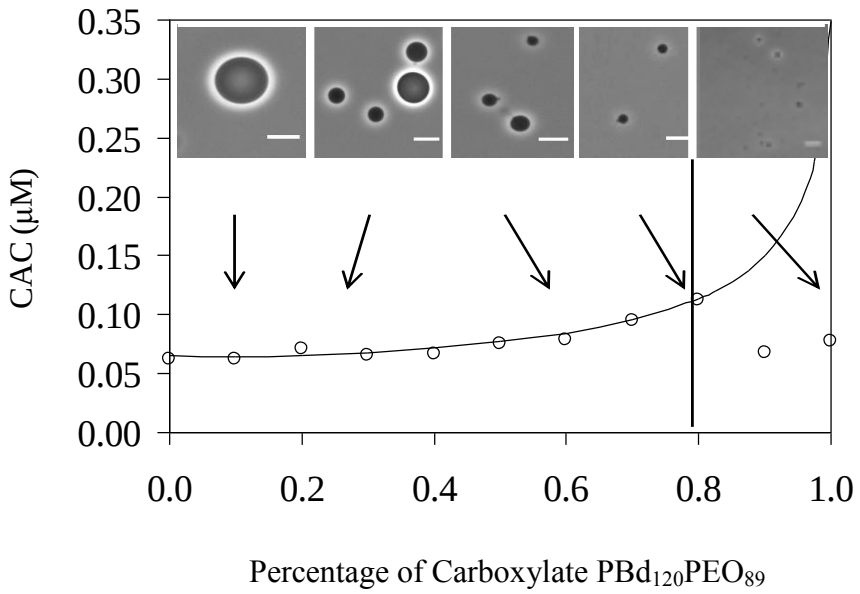

Figure 2.4 CAC of carboxylate $PBd_{120}PEO_{89}$ and unmodified $PBd_{120}PEO_{89}$ mixture. As the carboxylate $PBd_{120}PEO_{89}$ content is increased, the CAC increases and the averaged size of vesicles formed decreases. The solid line represents the theoretical CAC^{mix} values while the open dots represent the experimental values obtained. These two sets of values match until an approximate 80% of carboxylate $PBd_{120}PEO_{89}$ is present in the mixture. The scale bar in all pictures represents 10μm.

When the composition exceeds 80%, the CAC trend is disrupted and in contrast to the theoretical predicted ideal case (solid curve), the experimental values drop down close to the corresponding values of the unmodified block copolymer. The phase contrast images insets of Figure 2.4 indicate the decrease of the corresponding average vesicle size as the percentage of carboxylate $PBd_{120}PEO_{89}$ increases. In the 100% case no vesicle formation was observed.

For aggregate formation, the transition between a single amphiphilic block copolymer (monomer) and a micelle (*n*-mer) can be considered in equilibrium, which is

known as the *mass action model* or the *pseudo-phase separation model*. The chemical potential of component *i* can be calculated as following with μ_i for monomerically and ideally solubilized phase in solution and μ_i^M for component *i* in a binary micelle [88-89]:

Phase one (monomeric): $$\mu_i = \mu_i^0 + RT\ln(C_i^m) \quad (1)$$

Phase two (in micelle): $$\mu_i^M = \mu_i^{M_0} + RT\ln(f_i \cdot x_i) \quad (2)$$

and, $$\mu_i^{M_0} = \mu_i^0 + RT\ln(C_i) \quad (3)$$

where $\mu_i^{M_0}$ is the chemical potential of component *i* in a homogenous aggregate, f_i is the activity coefficient specifying the nonideality of the mixture, x_i is the mole fraction of copolymer *i* in the binary micelle, C_i^m is the concentration of *i* in the solution, and C_i is the critical micelle concentration of component *i* in solution.

At phase equilibrium $\mu_i = \mu_i^M$, which yields

$$x_i = \frac{C_i^m}{f_i C_i} \quad (4)$$

Since we have

$$C_i^m = \alpha_i C^{mix} \quad (5)$$

i.e., the CAC concentration of monomer *i* (C_i^m) is equal to the mole fraction of polymer *i* in the mixture (α_i) times the mixed CAC (C^{mix}). This equation in combination with equation 4 and the relationship of mole fraction between components *I* =1,2 ($1 = x_1 + x_2$) yields

$$1 = \frac{\left(\alpha_1 C^{mix}\right)}{f_1 C_1} + \frac{\left(\alpha_2 C^{mix}\right)}{f_2 C_2} \tag{6}$$

Since we are not dealing with an ideal binary mixture, the equations require the following activity coefficients:

$$f_1 = \exp\left[\beta(1-x_1)^2\right] \tag{7}$$

$$f_2 = \exp(\beta x_1^2) \tag{8}$$

where x_1 carboxylate $PBd_{120}PEO_{89}$ and β is an empirical parameter that represents the intermolecular interaction between components 1 and 2. x_i can be found by minimization of the total Gibbs free energy for the micelle and the solutions are

$$G_N^M = Nx_1\mu_1^M + Nx_2\mu_2^M \tag{9}$$

$$G_N = Nx_1\mu_1 + Nx_2\mu_2 \tag{10}$$

where N is the number of moles. Thus, the total change in free energy of the micelle during micellation is the potential difference between the micelle phase and the monomeric phase:

$$\Delta G_N^M = Nx_1(\mu_1^M - \mu_1) + Nx_2(\mu_2^M - \mu_2) \tag{11}$$

After manipulation, the resulting equation 12 can be used to find the concentration of polymer 1 in the aggregate (x_1).

$$\ln\left[\frac{(1-x_1)C_2}{x_1C_1}\right] = \beta(1-2x_1) + \ln\left(\frac{1-\alpha_1}{\alpha_1}\right) \tag{12}$$

After iterating equation 12 for x_i, it is substituted into equation 6 to find the CAC^{mix}, which is plotted as a solid line in Figure 2.3. The β value [87] for carboxylated PBdPEO were adjusted until the calculated CAC values fit the data, β = -2.01.

Below 80% of carboxylate $PBd_{120}PEO_{89}$ in the mixture, the experimental values confirm the theoretical prediction. After 80%, the CAC trend is disrupted and only very small vesicles are formed (unmodified polymer still present but in a very low concentration, less than 20%). This can be explained by the lower solubility of the carboxylate $PBd_{120}PEO_{89}$ which leads to their precipitation.

2.8 Conclusions

The primary alcohol end group of a diblock copolymer is chemically modified and effectively combined with unmodified block copolymer to form stable functionalized polymeric vesicles. The free hydroxyl terminal end group of the block copolymer Poly(butadiene-b-ethylene oxide) ($PEO_{89}PBd_{120}$, MW 10400 g/mol) is oxidized to its corresponding carboxylic acid (carboxylate $PBd_{120}PEO_{89}$) through a selective two phase oxidation reaction while other oxidizable groups remain unaffected.

The CAC values of vesicle solutions containing a mixture of carboxylate $PBd_{120}PEO_{89}$ and unmodified $PBd_{120}PEO_{89}$ increase when the percentage of carboxylate $PBd_{120}PEO_{89}$ is increased, while the average vesicle size decreases. They are consistent with the observation that the carboxylic acid presence disrupts the vesicle formation process, hence not being able to be incorporated into an unmodified block copolymer membrane at concentrations higher than 80% are reached.

CHAPTER III

COVALENT COUPLING OF PRIMARY AMINE TO CARBOXYLATE PBd_{120}-PEO_{89} DIBLOCK COPOLYMER

3.1 Overview

Three different primary amines were linked to the carboxylate derivative of the diblock copolymer polybutadiene-b-poly(ethylene oxide) ($PBd_{120}PEO_{89}$, MW 10400 g/mol), **(2)**, by developing an amination reaction that was carried out in an organic solvent. This straightforward reaction successfully formed a covalent bond (peptide linkage) between the carboxylic acid and the amines giving products **(3)**, **(4)** and **(5)** (see Figure 3.3). The location of the primary amine was determined, hence, it was corroborated that these amine are located at the vesicles surface. These functionalized derivatives were effectively incorporated into vesicles' bilayer and surface density control was achieved.

3.2 Introduction

Chemical labeling and surface modification of diblock copolymer vesicles are of interest due to their potential use as drug delivery systems or mimics of living cells. EDC/NHS covalent coupling reaction [90-92] has been widely used to prepare amine-reactive esters of carboxylate groups. Carboxylate groups (R-COOH) react with EDC (1-Ethyl-3-[3-dimethylaminopropyl] carbodiimide hydrochloride) to form an amine

reactive *O*-acylisourea intermediate. In the presence of NHS (*N*-Hydroxysuccinimide) this intermediate can be stabilized being converted into an amine-reactive NHS ester and, if a primary amine is present (R'-NH_2), the semi-stable NHS ester will react with it to form a stable amide bond (R-CONH-R') [93-95]. This linking chemistry is commonly used in protein and cell studies and it is usually performed in an aqueous environment for that reason.

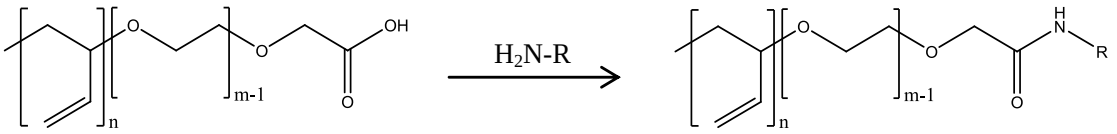

Figure 3.1 Covalent coupling reaction of primary amine to carboxylate $PBd_{120}PEO_{89}$ diblock copolymer. The respective functionalized diblock copolymer is produced after a primary amine (R = 6AF, COU or NA) is linked to its carboxylate form.

However, due to the amphiphilic nature of the diblock copolymers used in this research, a different approach was necessary and an organic environment was chosen to perform this reaction. A number of organic solvents were evaluated, including methanol, ethanol, dichloromethane, tetrahydrofuran, toluene as well as mixtures of them but, a 1:1 mixture of methanol:chloroform (MeOH:$CHCl_3$) was the one that gave the best results. This adaptation will allow the diblock copolymer and other reactants to dissolve completely to form a homogeneous reaction mixture.

After synthesizing product **(2)** as described in Chapter II, a subsequent amination reaction was conducted in the organic phase (1:1 MeOH:$CHCl_3$). The free terminal

hydroxyl group of the carboxylated $PBd_{120}PEO_{89}$ diblock copolymer was covalently linked to a primary amine through the EDC/NHS coupling. Figure 3.1 shows the general structure of the obtained functionalized block polymer ($PBd_{120}PEO_{89}$-R). The following functionalized block copolymers were obtained: $PBd_{120}PEO_{89}$-6AF, $PBd_{120}PEO_{89}$-COU and $PBd_{120}PEO_{89}$-NA. The chemical structures of the three different primary amines used: 6-amino-fluorescein (6AF), 7-amino-4-(trifluoromethyl) coumarin (COU) and the hormone DL-Noradrenaline hydrochloride (NA) are shown in Figure 3.2.

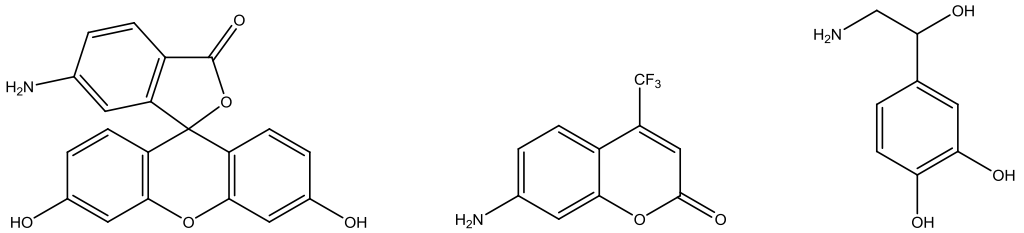

6AF COU NA

Figure 3.2 Structure of the three different primary amines used for the functionalization of carboxylate $PBd_{120}PEO_{89}$ diblock copolymer. From left to right: 6-amino-fluorescein (6AF), 7-amino-4-(trifluoromethyl) coumarin (COU) and DL-Noradrenaline (NA).

The covalent coupling was conducted at room temperature using the organic solvent, under an inert gas atmosphere to prevent degradation of susceptible reactants and under constant agitation. Figure 3.3 describes the synthetic pathway followed to produce three functionalized diblock copolymers. The carbodiimide EDC, NHS and the carboxylate diblock copolymer were first mixed in the organic solvent for 15 minutes prior to the addition of the primary amine. Then, the primary amine of interest was

added to the reaction vessel under constant stirring at 900 rpm and reacted for 2 hours. The amine-reactive NHS ester (stable intermediate) reacted with the amine and formed a stable amide bond. Multiple additions of EDC/NHS (2 hours apart) were performed to increase the final product yield and the reaction was run overnight for 24 hours.

After achieving the synthesis of the fluorophore (6AF and COU) and hormone (NA) functionalized diblock copolymers, they were successfully incorporated into vesicle's bilayer of unreacted $PBd_{120}PEO_{89}$ at a 1:9 ratio. The fluorescently labeled polymers were studied using fluorescent microscopy which led to confirm the efficacy of the linking chemistry proposed. Fluorescent spectroscopy helped to elucidate that the fluorophore molecule was actually located at the surface of the vesicle bilayer instead of any other possible sites such as the hydrophobic bilayer region or just dissolved in solution. The two fluorescently label diblock copolymers were also combined in the same vesicle structure. The concentration of each labeled polymer can be changed and it was shown that surface density can be controlled.

The hormone labeled polymer ($PBd_{120}PEO_{89}$-NA) was characterized by UV-Vis spectroscopy and used with cultured cells to verify an intracellular response to the drug molecule transported to the surface of the functionalized vesicle later on (see Chapter IV).

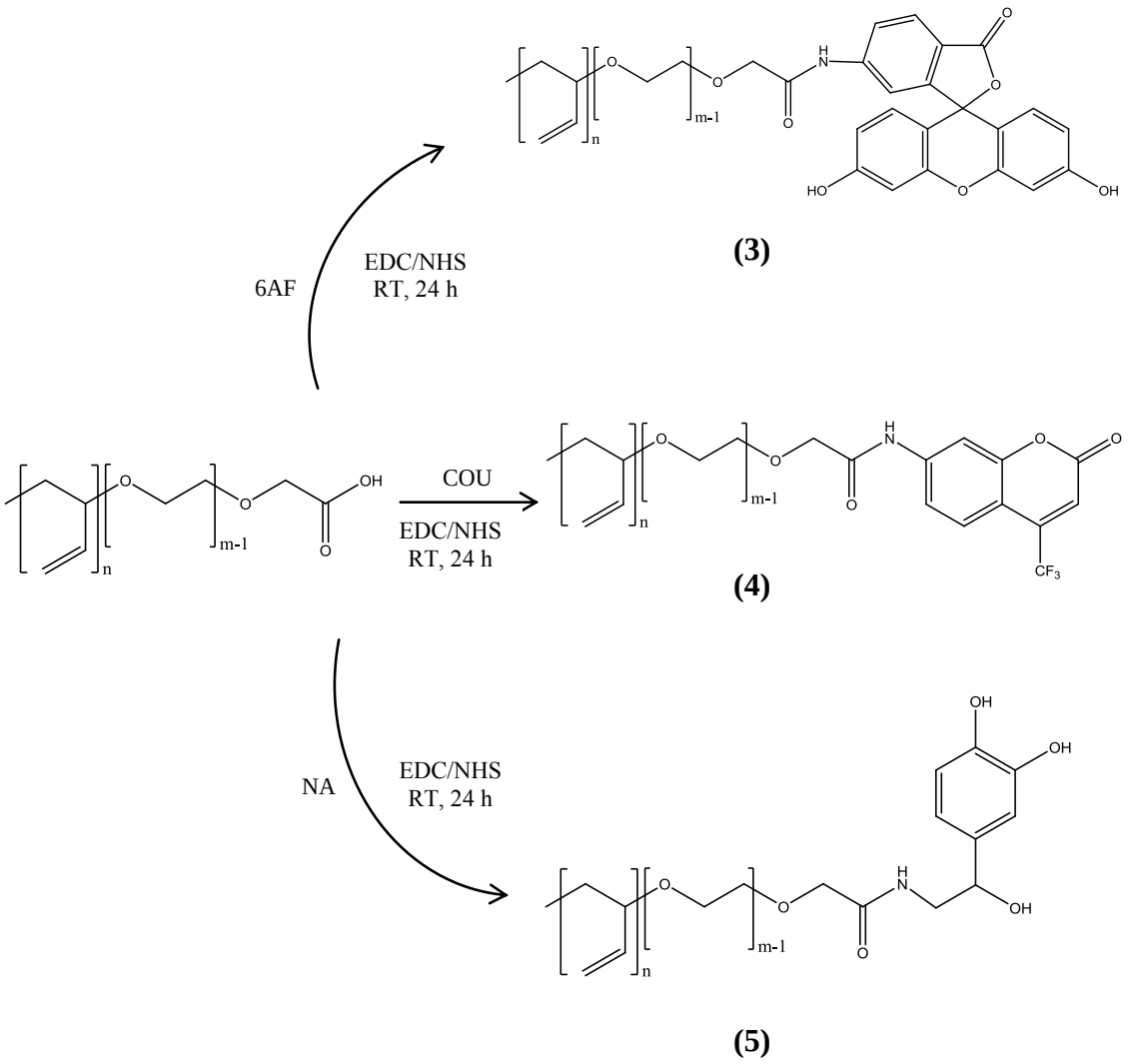

Figure 3.3 Synthetic pathway for functionalized diblock copolymers: **(3)** $PBd_{120}PEO_{89}$-6AF, after amination reaction with 6AF; **(4)** $PBd_{120}PEO_{89}$-COU, after amination reaction with COU; **(5)** $PBd_{120}PEO_{89}$-NA, after amination reaction with NA. Products were obtained by EDC/NHS covalent coupling of carboxylate $PBd_{120}PEO_{89}$ diblock to the respective primary amine.

3.3 Materials

$PBd_{120}PEO_{89}$ (MW 10400 g/mol) diblock copolymer and sucrose (ACS reagent) ($C_{12}H_{22}O_{11}$, MW 342.3 g/mol) were purchased from Polymer Source Inc. (Canada) and

Fisher Scientific (Pittsburgh, PA), respectively. Dichloromethane (anhydrous, 99.9%) (CH_2Cl_2, MW 84.93 g/mol), chloroform (99.8+% for analysis ACS, stabilized with ethanol) ($CHCl_3$, MW 119.38 g/mol) and methanol (99.8+% for analysis ACS) (MeOH, MW 32.04 g/mol) were purchased from Acros Organics (Morris Plains, NJ). 7-amino-4-(trifluoromethyl) coumarin (COU, MW 229.16 g/mol) and tetrahydrofuran (≥ 99.0% ACS reagent) (THF, MW 72.11 g/mol) were purchased from Sigma-Aldrich (St. Louis, MO). 6-amino-fluorescein (6AF, MW 347.32 g/mol) and DL-Noradrenaline hydrochloride (NA, MW 205.64 g/mol) were purchased from Fluka (Switzerland). 1-Ethyl-3-[3-dimethylaminopropyl]carbodiimide hydrochloride (EDC, MW 191.70) and *N*-Hydroxysuccinimide (NHS, MW 115.09 g/mol) were purchased from Pierce (Rockford, IL). Regenerated cellulose dialysis tubing kit (MWCO 8000 g/mol) was purchased from Spectra/Por®Biotech and, the previously synthesized carboxylate PBd_{120}-PEO_{89} diblock copolymer.

3.4 Experimental Methods

Diblock Copolymer Characterization

IR Spectroscopy. IR spectra of neat liquids were performed using a Bruker FT-IR TENSOR™ spectrometer (Billerica, MA) equipped with OPUS™ measurement software. Potassium bromide salt plates (McCarthy Scientific Co., Fallbrook, CA) and CH_2Cl_2, or $CHCl_3$, were used to evaluate the polymer samples.

UV-Vis Absorbance Measurements. Absorbance measurements of the obtained PEO_{89}-PBd_{120}-NA were performed using a Shimadzu UV-Mini 1240 spectrophotometer (Columbia, MD). Quartz cuvettes (1 cm pathlenght) and $CHCl_3$ were used as sample holder and solvent respectively. Free PEO_{89}-PBd_{120}-NA dissolved in $CHCl_3$ and the respective sets of controls were also analyzed by UV-Vis Spectroscopy.

Vesicle Solution Characterization

Cross-Polarizing Fluorescent Microscopy. Vesicle solutions were imaged using the temporary closed sample chamber described before. Phase contrast images of polymersomes were taken by a Carl Zeiss Axiovert 200M inverted microscope with 100 W HBO Mercury vapor lamp coupled to a Zeiss AxioCam MRm camera and a 20X objective (numerical aperture of 0.5). Fluorescent microscope images were obtained using a FITC band-pass filter with an excitation wavelength of 475 nm (bandwidth of 40 nm) and an emission wavelength of 530 nm (bandwidth of 50 nm); or a DAPI low-pass filter with an excitation wavelength of 365 nm, and an emission wavelength of 445 nm (bandwidth of 50 nm). Vesicle solutions of controls and samples containing 10% w/w of $PEO_{89}PBd_{120}$-6AF or, $PEO_{89}PBd_{120}$-COU, and 90% of unmodified $PEO_{89}PBd_{120}$ were prepared and imaged under fluorescence microscopy. To facilitate comparison of samples to controls, all images were taken sequentially using the same instrumental parameters and the recorded images were processed and analyzed identically with the program ImageJ.

Confocal Microscopy. Confocal images of vesicles containing PEO_{89}-PBd_{120}-6AF were recorded using a Leica TCS SP5 broad band confocal microscope (Bannockburn, IL). Pictures were taken at a scan rate of 400 Hz using a 63X oil objective. A 488 nm excitation laser and a 500-600 nm opening emission were used as well as a 700V photo multiplier tube power and a 100μm pinhole.

Fluorescence Spectroscopy. Steady-state excitation and emission spectra were recorded on a Photon Technology International (PTI) (Birmingham, NJ) QuantaMaster™ UV VIS spectrofluorometer equipped with FeliX32™ software package. During vesicle sample measurements, one polarizer was placed before the sample and the analyzer placed before the emission collection compartment was rotated to a perpendicular angle with respect to the excitation polarizer to reduce intense scattering from the polydisperse vesicle sample. This configuration allows the fluorescence of the vesicle system to be recorded.

In order to determine the location of fluorophore molecules in a vesicle solution different environments were simulated by dissolving COU in different solvents: (A) aqueous 0.15M PBS solution and the respective excitation and emission spectra were recorded at 375 and 490 nm; (B) decane and the excitation and emission spectra were recorded at 350 and 400 nm respectively; (C) aqueous 15% w/w PEO (MW 2000 g/mol) solution and the excitation and emission spectra were recorded at 385 and 490 nm respectively, and finally (D) a vesicle solution containing 10% $PBd_{120}PEO_{89}$-COU is prepared in an aqueous 0.3M sucrose media and the same excitation and emission wavelengths used for case (A) were applied here.

3.5 Synthesis of Functionalized Diblock Copolymer

The reactions were conducted under an argon atmosphere and stirred at 900 rpm using a Teflon-covered stir bar. A 5 mL reaction flask was charged with 1 mL of 1:1 MeOH:$CHCl_3$ solution of $1x10^{-3}$ mmol carboxylate $PBd_{120}PEO_{89}$, $10x10^{-3}$ mmol of EDC (dissolved in $CHCl_3$) and $5x10^{-3}$ mmol of NHS (dissolved in THF). The mixture was allowed to react for 15 minutes at room temperature. A primary amine (6AF, COU or NA) in a 5 fold excess was dissolved in 1:1 MeOH:$CHCl_3$, added to the reaction flask and allowed it to react for 2 hours under constant magnetic stirring. Extra doses of EDC and NHS were added every two hours to increase amount of amine linked to carboxylate groups. After the cleaning procedure, the final product was dried out in a vacuum oven redisolved in CH_2Cl_2 and an aliquot of the reaction solution was evaporated on a NaCl plate and respective the IR spectrum was obtained.

Synthesis of Diblock Copolymer Controls

The modified diblock copolymers used in controls and samples were prepared using different components and were labeled as follow: Control 1: When $PBd_{120}PEO_{89}$, EDC, NHS and a primary amine (6AF, COU or NA) were combined; control 2: when carboxylate $PBd_{120}PEO_{89}$ and a primary amine (6AF, COU or NA) were combined; sample: when carboxylate $PBd_{120}PEO_{89}$, EDC, NHS and a primary amine (6AF, COU or NA) were combined.

Synthesis of (3)

Carboxylate $PBd_{120}PEO_{89}$ (30.40 mg, $2.92x10^{-3}$ mmol), EDC (5.60 mg, $29.23x10^{-3}$ mmol), NHS (1.68 mg, 14.62 $x10^{-3}$ mmol) and 6AF (5.08 mg, $14.62x10^{-3}$ mmol) were reacted in methanol/chloroform as described above. In this manner, product **3** (24.62 mg, 81% yield) was obtained. IR (ν): 1703 (C=O) cm^{-1}, 1539 (N-H bend) cm^{-1}.

Synthesis of (4)

Carboxylate $PBd_{120}PEO_{89}$ (30.40 mg, $2.92x10^{-3}$ mmol), EDC (5.60 mg, $29.23x10^{-3}$ mmol), NHS (1.68 mg, 14.62 $x10^{-3}$ mmol) and COU (3.35 mg, $14.62x10^{-3}$ mmol) were reacted in methanol/chloroform as described above. In this manner, product **4** (23.41 mg, 77% yield) was obtained. IR (ν): 1703 (C=O) cm^{-1}, 1558 (N-H bend) cm^{-1}.

Synthesis of (5)

Carboxylate $PBd_{120}PEO_{89}$ (30.40 mg, $2.92x10^{-3}$ mmol), EDC (5.60 mg, $29.23x10^{-3}$ mmol), NHS (1.68 mg, 14.62 $x10^{-3}$ mmol) and NA (3.01 mg, $14.62x10^{-3}$ mmol) were reacted in methanol/chloroform as described above. In this manner, product **5** (21.89 mg, 72% yield) was obtained. IR (ν): 1700 (C=O) cm^{-1}, 1538 (N-H bend) cm^{-1}.

Functionalized Diblock Copolymer Cleaning Procedure

The desired product, was redisolved in 2 mL of a 1:1 MeOH:$CHCl_3$ solution and cleaned using regenerated cellulose dialysis tubing (MWCO 8000 g/mol). The sample

was dialyzed for 2 hours at room temperature against 600 mL (300 times the volume of the sample) of 1:1 MeOH:$CHCl_3$ solution, the dialysis buffer was changed and the sample dialyzed for another 2 hours. Finally, the dialysis buffer was changed for the second time and the sample dialyzed overnight.

3.6 Vesicle Solution Preparation

A polymer film containing 100 μg of the desired block copolymer or block copolymer mixture was formed by evaporation (8 hours) at the bottom of a 5 mL glass scintillation vial. Polymersomes were formed by rehydration of this polymer film during 24 hours at 60ºC with 2 mL of 300 mOsm/kg sucrose solution. In the case of vesicles formed with a mixture of block copolymers, X% w/w of functionalized $PBd_{120}PEO_{89}$ block copolymer was ideally mixed with Y% w/w of unmodified $PBd_{120}PEO_{89}$ block copolymer before the polymer film formation step. Vesicle solutions of the following mixture compositions were formed: 10% w/w of $PBd_{120}PEO_{89}$-6AF and 90% w/w of unmodified $PBd_{120}PEO_{89}$, 10% w/w of $PBd_{120}PEO_{89}$-COU and 90% w/w of unmodified $PBd_{120}PEO_{89}$ and, 10% w/w of $PBd_{120}PEO_{89}$-NA and 90% w/w of unmodified $PBd_{120}PEO_{89}$. The final block copolymer concentration in a vesicle solution of 2 mL is 4.8 μM.

Similarly, vesicle solutions of the following mixture compositions (also using a 300 mOsm/kg sucrose solution) were prepared for surface density control experiments: 2.5% w/w of $PBd_{120}PEO_{89}$-COU and 90% w/w of unmodified $PBd_{120}PEO_{89}$, 5.0% w/w of $PBd_{120}PEO_{89}$-6AF, 5.0% w/w of $PBd_{120}PEO_{89}$-COU and 90% w/w of unmodified

$PBd_{120}PEO_{89}$ and, 2.5% w/w of $PBd_{120}PEO_{89}$-6AF, 7.5% w/w of $PBd_{120}PEO_{89}$-COU and 90% w/w of unmodified $PBd_{120}PEO_{89}$.

Vesicle Solution for Fluorescence Spectroscopy

The vesicle solution used for fluorescence measurements was prepared using a 300 mOsm/kg sucrose solution, 10% w/w of $PBd_{120}PEO_{89}$-COU and 90% w/w of unmodified $PBd_{120}PEO_{89}$.

Vesicle Solution Controls

Vesicle solutions of controls and samples were prepared by combining in a 9:1 ratio the unreacted $PBd_{120}PEO_{89}$ and the functionalized diblock copolymer.

3.7 Results and Discussion

Synthesis of (3)-(5)

The EDC/NHS amination reactions effectively produced compounds (3), (4) and (5) and yields ≥ 70% were obtained in all cases.

Verification of Product (3)-(5) Composition

Figure 3.4 compares the spectrum of the unmodified $PBd_{120}PEO_{89}$ to that of $PEO_{89}PBd_{120}$-6AF, $PEO_{89}PBd_{120}$-COU and $PEO_{89}PBd_{120}$-NA. The presence of a carbonyl stretch peaks (1730 cm^{-1}) and N-H bend peaks (1540 cm^{-1}) in each IR spectra

demonstrates the formation of a secondary amide linkage between the carboxylate $PBd_{120}PEO_{89}$ and the respective primary amine.

Imaging of 6AF Functionalized Vesicles

Figure 3.5 shows a set of images of polymersomes made up with 90% $PBd_{120}PEO_{89}$ and 10% $PBd_{120}PEO_{89}$-6AF following a standard vesicle formation procedure in a 310 mOsm/kg sucrose solution. Figure 3.5(A) shows a phase contrast microscopy image of a well defined vesicle and Figure 3.5(B) shows the same vesicle is observed under fluorescent light (FITC filter) where, the fluorescent vesicle membrane can be clearly seen as a bright ring after focusing in its middle plane. The confocal image shown in Figure 3.5(C) is a side view of a fluorescent vesicle sitting over a cover glass and it is evident that the fluidity of the polymer membrane is preserved. These images corroborate that the carboxylate $PBd_{120}PEO_{89}$ reacted with 6AF (fluorescent) to form the corresponding amide ($PBd_{120}PEO_{89}$-6AF) and that modified block copolymers were successfully incorporated into the vesicles without disrupting its original morphology and characteristics such as membrane fluidity.

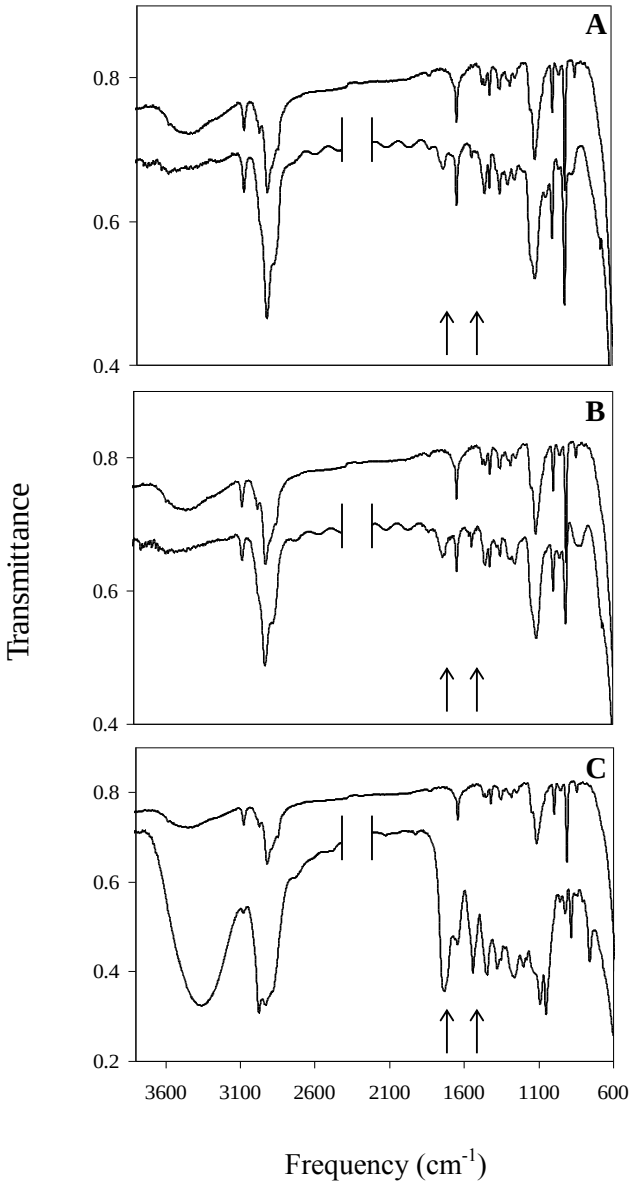

Figure 3.4 Comparison between the IR spectra of the unmodified $PBd_{120}PEO_{89}$ and the covalent coupling reaction products from the respective carboxylate block copolymer, 6-amino-fluorescein $PBd_{120}PEO_{89}$ ($PBd_{120}PEO_{89}$-6AF), 7-amino-4-(trifluoromethyl) coumarin PBd_{120}-PEO_{89} ($PBd_{120}PEO_{89}$-COU) and DL-Noradrenaline $PBd_{120}PEO_{89}$ ($PBd_{120}PEO_{89}$-NA). Overlay of IR spectra showing: (A) $PBd_{120}PEO_{89}$ (top) and $PBd_{120}PEO_{89}$-6AF product. (B) $PBd_{120}PEO_{89}$ and $PBd_{120}PEO_{89}$-COU product. (C) $PBd_{120}PEO_{89}$ and $PBd_{120}PEO_{89}$-NA product. The presence of a carbonyl stretch (around 1700 cm^{-1}) and a peak corresponding to a N-H bend (around 1530 cm^{-1}) indicates the formation of an amide bond between the block copolymer and the primary amines.

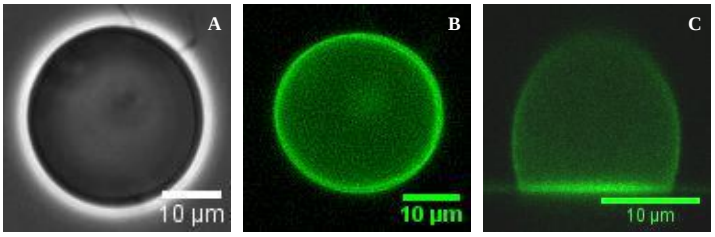

Figure 3.5 Block copolymer vesicles of 10% $PBd_{120}PEO_{89}$-6AF and 90% $PBd_{120}PEO_{89}$. (A) Phase contrast image. (B) Fluorescent image taken using FITC filter. (C) Side view image obtained by confocal microscopy.

Fluorescent Microscopy Analysis of Functionalized Vesicles

Figure 3.6 and Figure 3.7 demonstrate through a set of controls and samples the effectiveness of the covalent coupling reaction of primary amines to the carboxylate end groups of carboxylate $PBd_{120}PEO_{89}$. For 6AF, phase contrast images of three types of vesicles (control 1, control 2 and sample) are shown in Figure 3.6(A) while the respective fluorescent images, taken using a FITC filter, can be observed in Figure 3.6(B). All the images were recorded consecutively and analyzed using the same microscope settings in order to minimize effects due to fluorescent lamp intensity or image processing. Table 3.1 shows the peak and average values of the vesicle's intensity profiles of controls and samples for the 6AF case. Three different vesicle sets were analyzed and in each case peak 1 and 2 correspond to both sides of the vesicle's bilayer observed on the transversal cut images obtained through fluorescent microscopy. Similarly, Table 3.2 shows the peak and average values of the vesicle's intensity profiles of controls and samples for the COU case.

Table 3.1 Intensity profile values of controls and samples of $PBd_{120}PEO_{89}$-6AF functionalized vesicles.

	Control 1 (Intensity units)			Control 2 (Intensity units)			Sample (Intensity units)		
	Peak 1	**Peak 2**	**Average**	**Peak 1**	**Peak 2**	**Average**	**Peak 1**	**Peak 2**	**Average**
Trial 1	6.9	6.3	**6.6**	45.9	46.0	**45.9**	118.6	132.0	**125.3**
Trial 2	8.3	9.3	**8.8**	77.5	75.5	**76.5**	184.7	210.8	**197.8**
Trial 3	8.2	7.1	**7.6**	71.1	68.8	**69.9**	137.7	172.8	**155.3**
StDev			**1.1**			**16.1**			**36.4**

Table 3.2 Intensity profile values of controls and samples of $PBd_{120}PEO_{89}$-COU functionalized vesicles.

	Control 1 (Intensity units)			Control 2 (Intensity units)			Sample (Intensity units)		
	Peak 1	**Peak 2**	**Average**	**Peak 1**	**Peak 2**	**Average**	**Peak 1**	**Peak 2**	**Average**
Trial 1	23.9	16.0	**19.9**	50.8	50.5	**50.6**	310.8	314.8	**312.8**
Trial 2	26.0	24.0	**25.0**	47.0	46.0	**46.5**	306.0	302.0	**304.0**
Trial 3	13.6	11.0	**12.3**	34.7	32.9	**33.8**	186.7	191.0	**188.9**
StDev			**6.4**			**8.8**			**69.1**

Control 1 lacks a carboxyl group at the end of the block copolymer chain. In the case of control 2, amide bonds could form due to the presence of a free primary amine (6AF) and the carboxylate $PBd_{120}PEO_{89}$. It can clearly be observed that the sample exhibits higher fluorescence intensity than both controls which indicates a higher percent of conversion for the coupling reaction product ($PBd_{120}PEO_{89}$-6AF). Figure 3.6(C) confirms the differences in fluorescent intensities for the two controls and the sample.

In the COU case, the same types of block copolymer vesicles were prepared (control 1, control 2 and sample) and fluorescent images were recorder using a DAPI filter. Comparable results to the 6AF case are obtained and shown in Figure 3.7. Since

there is no carboxyl group present in control 1, and the slight fluorescence of control 2 suggests the formation of only few amide bonds, the higher fluorescence intensity exhibited by the sample indicates a higher percent conversion for the coupling reaction between the carboxylate $PBd_{120}PEO_{89}$ and COU.

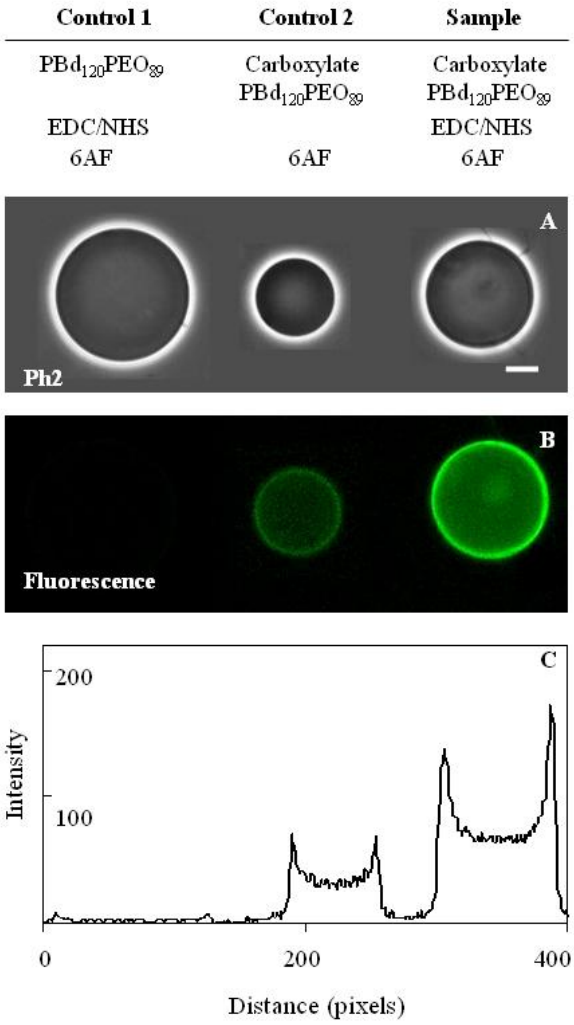

Figure 3.6 Images of fluorescent block copolymer vesicles from $PBd_{120}PEO_{89}$ and $PBd_{120}PEO_{89}$-6AF mixed at 9:1 ratio. The table above explains the reactants used for controls and the sample. (A) Phase contrast images. (B) Fluorescent images taken using FITC filter. (C) Intensity profiles corresponding to each fluorescent vesicle shown in (B).

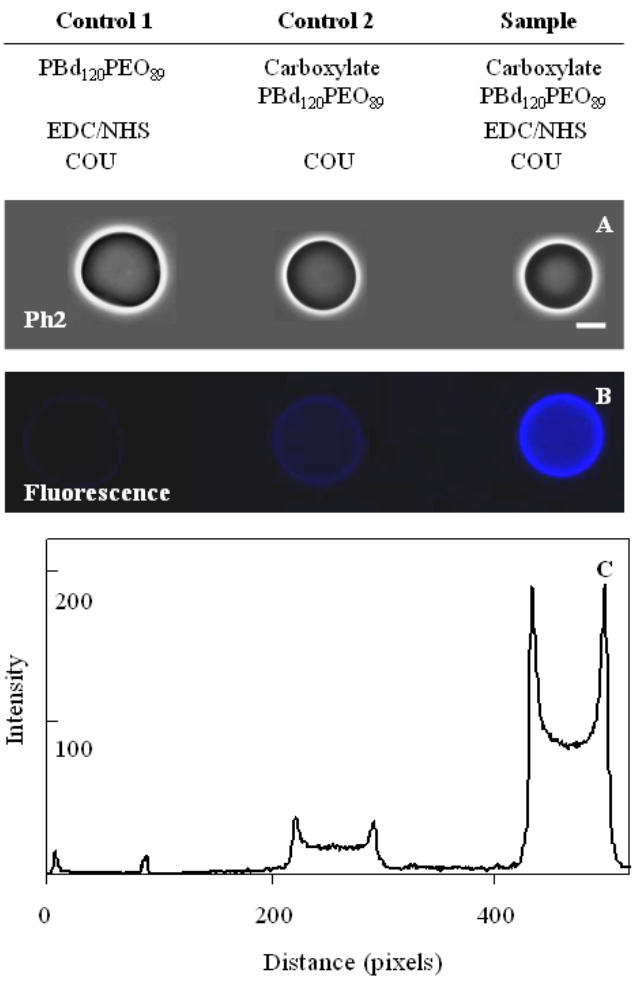

Figure 3.7 Images of fluorescent block copolymer vesicles from $PBd_{120}PEO_{89}$ and $PBd_{120}PEO_{89}$-COU mixed at 9:1 ratio. The table above explains the reactants used for controls and the sample. (A) Phase contrast images. (B) Fluorescent images taken using DAPI filter. (C) Intensity profiles corresponding to each fluorescent vesicle shown in (B).

UV-Vis Spectroscopy Analysis of Hormone Functionalized Diblock Copolymer

Figure 3.8 shows the concentration of $PBd_{120}PEO_{89}$-NA present in control 1, control 2 and sample determined by UV absorbance measurements of the respective free polymer dissolved in $CHCl_3$.

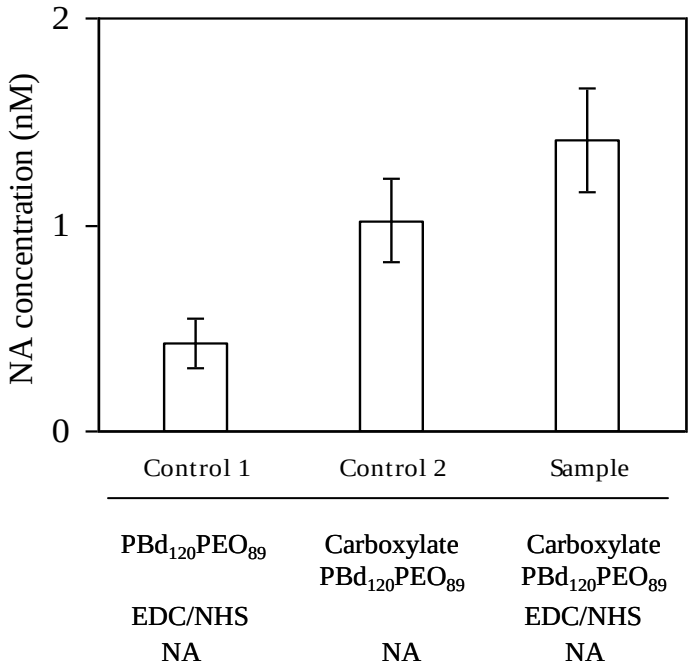

Figure 3.8 UV absorbance of block copolymer $PBd_{120}PEO_{89}$-NA in CHCl3 taken at λ=380 nm. Control 1 has no modified polymer. Control 2 has no coupling reagents. Sample shows the final product (73% conversion). Polymer concentrations are 1.9 mM.

A 1.9 mM carboxylate $PBd_{120}PEO_{89}$ solution is used for these amination reactions and the $PBd_{120}PEO_{89}$-NA yields obtained for control 1, control 2 and sample by UV absorbance measurements are 22, 53, and 73% respectively. Due to the lack of a carboxyl group in the block copolymer chain of control 1 no further reaction can occur however, amide bonds can be formed in control 2 due to the presence of a primary amine (NA) and the carboxylate $PBd_{120}PEO_{89}$. Lastly, the higher fluorescence exhibited by the sample indicates again a higher percent of conversion for the linking reaction between the carboxylate $PBd_{120}PEO_{89}$ and NA.

Fluorophore Localization Through Fluorescence Spectroscopy

In order to establish the actual location of the fluorescent primary amines used (6AF and COU) during the EDC/NHS coupling to the carboxylate $PBd_{120}PEO_{89}$, fluorescence measurements were conducted (Figure 3.9). The three possible locations where the fluorophores can be found are: (A) Free in aqueous solution, where no covalent coupling with the carboxylate $PBd_{120}PEO_{89}$ was achieved. (B) Free and solubilized in the hydrophobic region of the vesicle membrane, when no reaction has occurred and the free fluorophore is partially solubilized in the vesicle membrane. (C) Covalently attached to the carboxylate $PBd_{120}PEO_{89}$. With the aim of simulating these environments, COU was dissolved in three different solutions as described in the experimental section and compared to a vesicle solution containing 10% $PBd_{120}PEO_{89}$-COU.

Figures 3.9 (A-C) shows the resultant fluorescence spectra of these simulated environments while Figure 3.9(D) shows the fluorescence spectra of a vesicle solution formed with the functionalized $PBd_{120}PEO_{89}$-COU. The vesicle solution spectra (Figure 3.9(D)) does not match the results presented in Figures 3.9(A) or 3.9(B) while Figure 3.9(C) shows very similar emission and absorption peaks. These results indicate that the fluorophore is not in the hydrophobic region or free in solution, but associated with the PEO block of the polymer.

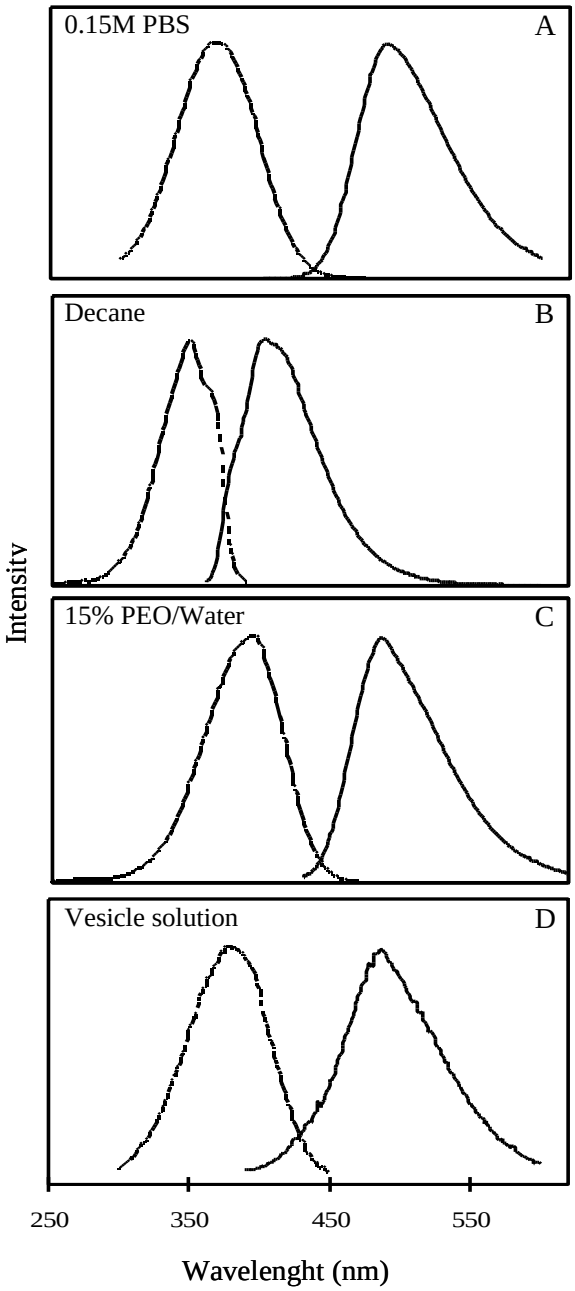

Figure 3.9 Fluorescent measurements of dissolved COU in different media simulating various environments (A) COU dissolved in an aqueous 0.15 M PBS solution. Excitation (375 nm) and emission (490 nm) were used respectively. (B) COU dissolved in decane. Excitation (350 nm) and emission (400 nm). (C) COU dissolved in an aqueous 15% w/w PEO (MW ~2000) solution. Excitation (385 nm) and emission (490 nm). (D) Vesicle solution of 10% $PBd_{120}PEO_{89}$-COU in an aqueous 0.3 M sucrose solution. Same excitation and emission wavelength used as in (A).

Surface Density Control of Functionalized $PBd_{120}PEO_{89}$-6AF and $PBd_{120}PEO_{89}$-COU in Diblock Copolymer Vesicles

Figure 3.10 shows the results of a surface density experiment were the amount and type of fluorescent $PBd_{120}PEO_{89}$, either linked to 6AF or COU, were controlled and deliberately modified. Block copolymer vesicles were formed using 90% $PBd_{120}PEO_{89}$ and 10% of a mixture of $PBd_{120}PEO_{89}$-6AF and $PBd_{120}PEO_{89}$-COU, ranging from a minimum of 2.5% to a maximum of 7.5% of each component.

These fluorescent microscope images were taken using separate FITC/DAPI filters. Each column represents one set of images of the same vesicle. Rows 1 and 2 show images taken with DAPI (to detect COU presence) and FITC (to detect 6AF presence) filter respectively and, while row 1 shows an increase in the $PBd_{120}PEO_{89}$-COU concentration from left to right (2.5%, 5.0% and 7.5% respectively), row 2 shows an increase in the $PBd_{120}PEO_{89}$-6AF concentration from right to left (2.5%, 5.0% and 7.5% respectively). Row 3 illustrates the superposition of the two previous images in the same column (actual image seen through the eye piece or microscope camera).

Images shown in column 1 correspond to a block copolymer vesicle made up with 7.5% $PBd_{120}PEO_{89}$-COU (Figure 3.10(A)) and 2.5% $PBd_{120}PEO_{89}$-6AF (Figure 3.10(D)). Column 2 present the images of a vesicle made up with 5.0% $PBd_{120}PEO_{89}$-COU (Figure 3.10(B)) and 5.0% $PBd_{120}PEO_{89}$-6AF (Figure 3.10(E)). Finally, column 3 displays the images of a vesicle made up with 2.5% $PBd_{120}PEO_{89}$-COU (Figure 3.10(C)) and 7.5% $PBd_{120}PEO_{89}$-6AF (Figure 3.10(F)).

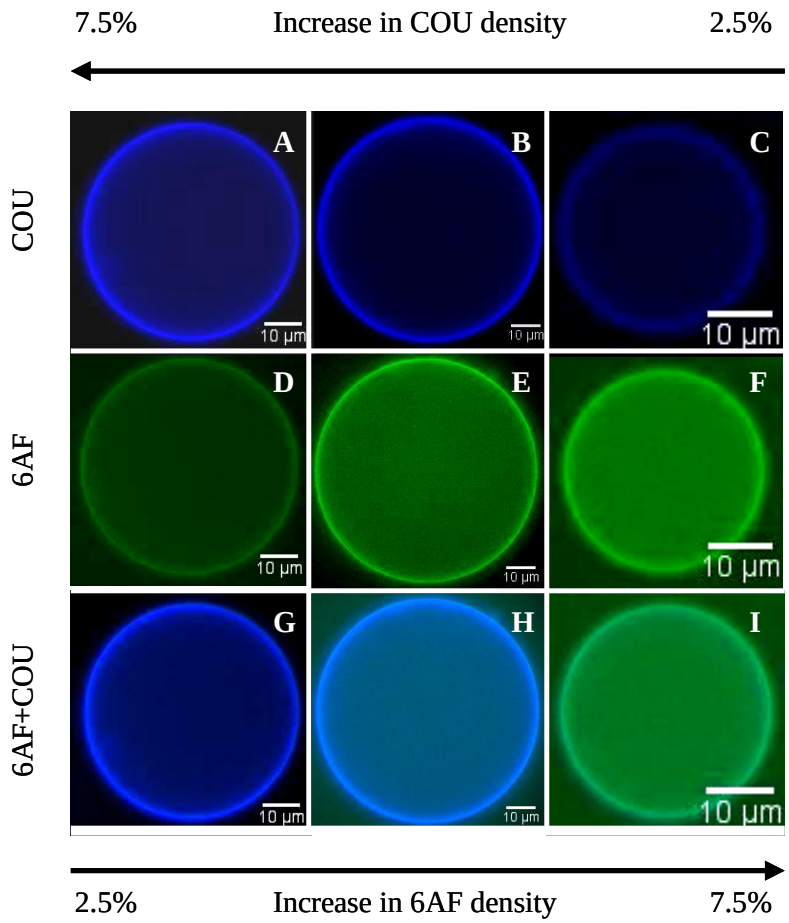

Figure 3.10 Surface density control of fluorescent block copolymer in polymersomes. 90% $PBd_{120}PEO_{89}$ and 10% of a mixture of $PBd_{120}PEO_{89}$-COU (A-C) and $PBd_{120}PEO_{89}$-6AF (D-F), ranging from a minimum of 2.5% to a maximum of 7.5% of each component. The combined or total fluorescence is shown in figures G-I. The amount and type of fluorescent $PBd_{120}PEO_{89}$ were tailored enabling us to exert surface density control of the vesicle components.

Figures 3.10(G-I) show the overlay of the respective upper images were the total fluorescence is constant while the blue and green vary with concentration. The overlay images of the COU and 6AF channels show the total fluorescence intensity of the three types of vesicles formed and demonstrate that the amount and type of functionalized

block copolymer incorporated into the vesicle can be tailored and that the surface density of a polymer vesicle can be accurately controlled.

3.8 Conclusions

Different primary amines were covalently attached to the previously synthesized carboxylate block copolymer through a modified amination reaction performed in organic phase. The peptide bond formation was confirmed through FT-IR spectroscopy and fluorescent microscopy. This constitutes a singular synthetic approach of this widely used coupling reaction due to the amphiphilic nature of the diblock copolymers that enable us to apply it to other molecule types.

Polymersomes containing 90% of the unmodified block copolymer and 10% of one of the modified block copolymers ($PBd_{120}PEO_{89}$-6AF, $PBd_{120}PEO_{89}$-COU, and $PBd_{120}PEO_{89}$-NA) were prepared and the effective incorporation of the latest one was demonstrated through fluorescence microscopy and UV absorbance measurements. Two types of modified diblock copolymers ($PBd_{120}PEO_{89}$-6AF, $PBd_{120}PEO_{89}$-COU) were also properly integrated into the same vesicle and, surface density control of the two fluorophores was achieved and confirmed through fluorescence microscopy.

This type of synthesis opens the possibility to produce different functionalized diblocks, with diverse uses and applications, which can be incorporated into the polymersome bilayer with the aim of safe transportation and further targeted delivery of the desired molecule.

CHAPTER IV

CELL RESPONSE TO HORMONE FUNCTIONALIZED $PBd_{120}PEO_{89}$ DIBLOCK COPOLYMER VESICLES

4.1 Overview

After the successful synthesis of functionalized diblock copolymers that can be integrated into polymeric vesicles, as described in previous chapters shows that functionalized vesicles can interact with living cells to induce a cell response [96]. A series of control and samples were evaluated and compared. A functionalized vesicle with noradrenaline (NA) molecules attached to its surface was placed in close contact with a cell surface using micropipette aspiration technique. We observed that the delivered hormone was bound to the noradrenaline a-receptors located on the surface of smooth muscle cells (SMC) and produced the expected cell response confirmed by as an increase of fluorescence using fluorescent microscopy.

4.2 Introduction

Noradrenaline (NA), also called norepinephrine, is one of the principal hormones and neurotransmitters of the nervous system. The noradrenaline effects includes the activation of the sympathetic nervous system, which causes the raise of glucose concentration in blood, increase in blood pressure and heartbeat rate, and boost muscular power and resistance to fatigue [87, 97]. It may also cause exocytosis, adhesion of cells

to the extracellular matrix, dilation of pupils and dilation of air passages in the lungs, narrowing of blood vessels in non-essential organs, and even apoptosis.

Noradrenaline is produced by the adrenal gland located on top of the kidneys and stored in small vesicles. In the occurrence of an impulse at a nerve terminal, the noradrenaline containing vesicles are released. After noradrenaline is used, the residual NA molecules are oxidized to inactive material or restored for later use. Noradrenaline interacts with two types of cell membrane receptors, named ‘a’ and ‘b’. The b-receptors cause relaxation, whereas the a-receptors cause contraction of smooth muscle cells when activated. The interaction between noradrenaline and the cell surface receptors [97-99] occurs via a cascade reaction involving a number of secondary messengers that amplify the strength of the transmitted signal.

Due to the importance of well balanced presence of molecules of this hormone in human body, we developed here diblock copolymer vesicles capable of carrying noradrenaline molecules in their surfaces. These functionalize vesicles can bind to a-receptors of smooth muscle cells to restore blood pressure to normal in life threatening situations when it has dropped dangerously low (known as acute hypotension). Currently, noradrenaline is administered in solution through injection. But, the outflow of it from veins can cause death of the tissue around therein. Hence, a controlled distribution of the drug using functionalized vesicles may be an alternative medical treatment.

In company to smooth muscle cell contractions, there is a rise in serum calcium [22, 37] that enables us to monitor the cell response to the presence of noradrenaline.

Here, we chose to observe and image via fluorescent microscopy the intracellular increase of Ca^{2+} ions through their coupling to a fluorescent indicator, such as Fluo-4 AM [100-102]. The increase in fluorescence intensity was caused by a series of controls and samples placed in closed contact with rat aortic smooth muscle cell cultures. The Fluo-4 AM ester is an uncharged molecule that is permeable to cell membranes. Once inside the cell, it binds to Ca^{2+} ions, and can be imaged due to the strong fluorescence intensity produced when excited at 488 nm [43, 98].

4.3 Materials

Previously synthesized noradrenaline Poly(butadiene-b-ethylene oxide) (PBd_{120}-PEO_{89}-NA) block copolymer and rat aortic smooth muscle cells (RASMC). Sucrose (ACS reagent) ($C_{12}H_{22}O_{11}$, MW 342.3 g/mol) and DL-Noradrenaline hydrochloride (NA, MW 205.64 g/mol) were purchased from Fisher Scientific (Pittsburgh, PA) and Fluka (Switzerland), respectively. PBd_{120}-PEO_{89} and Poly(butadiene-b-ethylene oxide) ($PBd_{33}PEO_{20}$, MW 2700 g/mol) block copolymers were purchased from Polymer Source Inc. (Canada). Carboxylate-modified polystyrene microspheres (red fluorescent, 2 μm in diameter) were purchased from Molecular Probes™, Invitrogen (Carlsbad, CA). High quality dimethylsulfoxyde (DMSO) ($(CH_3)_2SO$, MW 78.13 g.mol) and Pluronic® F-127 were purchased from Sigma-Aldrich (St. Louis, MO). Dulbecco's Modified Eagle's Medium (DMEM) (4.5 g/L glucose, L-glutamine, sodium pyruvate) and Antibiotic-Antimycotic solution (10000 I.U./mL penicillin, 10000 μg/mL streptomycin, 25 μg/mL amphotericin B) were purchased from Cellgro®, Mediatech, Inc. (Herndon, VA).

Phosphate buffered saline 1X (PBS) and Bovine Calf Serum (BCS) were purchased from HyClone, Thermo Fisher Scientific, Inc. Fluo4 AM was purchased from Invitrogen (Carlsbad, CA).

4.4 Experimental Methods

Vesicle and Cell Characterization

Micropipette Aspiration. A single vesicle was hold close to a cultured cell using a micropipette aspirator. In this technique, vesicles were aspirated into a pipette of small inner diameter (approximate 8 μm) by applying suction pressure causing changes of the vesicle's membrane tension. This highly specialized technique required custom laboratory fabrication of glass micropipettes by a micropipette puller and a micro forge equipped with a microscope.

Microscope Imaging and Cross-Polarizing Fluorescent Microscopy. Cells and vesicles were imaged using an open Petri dish and a silicone rubber well as a vesicle chamber. Individual vesicles were hold using micropipette aspiration technique to place them in close contact with cell surface. Bright field images were taken via a 20X objective of a Carl Zeiss Axiovert 200M inverted microscope with 100 W HBO Mercury vapor lamp and recorded by a Zeiss AxioCam MRm camera. Fluorescent microscope images were obtained using a FITC band-pass filter with an excitation wavelength of 475 nm (bandwidth of 40 nm) and an emission wavelength of 530 nm (bandwidth of 50 nm). All images were recorded consecutively using the same microscope settings in

order to minimize effects due to fluorescent lamp intensity fluctuation or image processing. The recorded images were processed and analyzed with the program ImageJ.

In all cases, consecutive fluorescent images (50 to 150 frames) of the same RASMC culture region are taken every 2 seconds. In each case, three smaller areas were numbered and marked by a square in each image and the fluorescence intensity of the cells contained in these areas was as a function of time before and after the addition of controls and functionalized beads or vesicles.

Cell Seeding Procedure

RASMC were transferred into a 60x15 mm round Petri dish and a final volume of 5 mL was reached by adding DMEM. The cells were incubated at 37ºC for 2 days or until a confluent cell layer was obtained. The DMEM media was changed every 2 days and cells were reseeded every 4-5 days.

Cell Staining Procedure

A 2.5 mM Fluo4 AM stock solution was prepared by dissolving 50 µg of Fluo4 AM in 18 µL of a 20% Pluronic® F-127 solution prepared in DMSO (0.4 g of Pluronic® F-127 in 2 mL of DMSO). The stock solution was then diluted to a 2.5 µM Fluo-4 AM solution by adding 18 mL of PBS. The Petri dish containing the seeded cells was charged with 1 mL of the 2.5 µM Fluo-4 AM solution and exposed to it for 40 minutes at room temperature.

4.5 Synthesis of Hormone Functionalized Diblock Copolymer

The reactions were conducted under an argon atmosphere and stirred using a Teflon-covered stir bar.

Hormone Functionalized Polystyrene Microspheres

A 5 mL reaction flask was charged with 1 mL aqueous solution of the carboxylate-modified polystyrene microspheres, $10x10^{-3}$ mmol of EDC and $5x10^{-3}$ mmol of NHS. The reaction mixture was allowed to react for 15 minutes at room temperature and under constant magnetic stirring. NA in excess ($10x10^{-3}$ mmol) was added to the reaction flask and allowed it to react for 2 hours. Extra doses of EDC and NHS were added every two hours to increase amount of amine linked to carboxylate groups. The final clean product was resuspended in 1 mL of DMEM.

Polystyrene Microspheres Control Suspension

A control bead solution was prepared at the same time but without addition of linking agents. A 5 mL reaction flask was charged with 1 mL aqueous solution of the carboxylate-modified polystyrene microspheres and magnetically stirred for 15 minutes at room temperature. NA ($10x10^{-3}$ mmol) was added to the reaction flask and allowed it to react for 2 hours. The final clean product was resuspended in 1 mL of DMEM.

Functionalized Microspheres Cleaning Procedure

The reaction mixture was cleaned using microcentrifuge filtration tubes (0.22 μm pore size). The functionalized beads were resuspended in 1 mL aqueous solution using a vortex and then filtrated. This procedure was repeated 3 times per sample and blanks.

4.6 Vesicle Solution Preparation

A polymer film containing 100 μg of the desired block copolymer or block copolymer mixture was formed by evaporation (8 hours) at the bottom of a 5 mL glass scintillation vial. Polymersomes were formed by rehydration of this polymer film during 24 hours at 60ºC with 2 mL sucrose solution. A 340 mOsm/kg sucrose solution was used during the rehydration step because of the higher osmolality of DMEM (350 mOsm/kg). A vesicle solution of the following mixture composition was formed: 10% w/w of $PBd_{120}PEO_{89}$-NA and 90% w/w of unmodified $PBd_{33}PEO_{20}$. The final block copolymer concentration in a vesicle solution of 2 mL is 4.8 μM.

Vesicle Solution Controls

Vesicle solutions of controls and samples are prepared by combining in a 9:1 ratio the unreacted $PBd_{33}PEO_{20}$ and the functionalized diblock copolymer control 1 or control 2.

4.7 Results and Discussion

Six cell response experiments were performed and the fluorescence intensity increase caused by controls and samples was recorded (see Table 4.1). RASMC were directly exposed to: NA dissolved in sucrose solution (free NA); carboxylate-modified polystyrene microspheres (control A); carboxylate-modified polystyrene microspheres linked to NA (control B); vesicle made with 10% unreacted $PBd_{120}PEO_{89}$ and 90% unreacted $PBd_{33}PEO_{20}$ (control 1); vesicle made with 10% carboxylate $PBd_{120}PEO_{89}$ and 90% unreacted $PBd_{33}PEO_{20}$ (control 2) and, vesicle made with 10% $PBd_{120}PEO_{89}$-NA and 90% unreacted $PBd_{33}PEO_{20}$ (sample).

Table 4.1 Reactants used to prepare controls and sample products. In the case of vesicles, they were formed using a 9:1 ratio of $PBd_{33}PEO_{20}$ and functionalized polymer.

Free NA	**Control A (Microsphere)**	**Control B (Microsphere)**	**Control 1 (Vesicle)**	**Control 2 (Vesicle)**	**Sample (Vesicle)**
NA	NA	NA	NA	NA	NA
		EDC	EDC		EDC
		NHS	NHS		NHS
	Microsphere	Microsphere	Unreacted $PBd_{120}PEO_{89}$	Carboxylate $PBd_{120}PEO_{89}$	Carboxylate $PBd_{120}PEO_{89}$
NA	Microsphere	Microsphere-NA	Unreacted $PBd_{120}PEO_{89}$	Carboxylate $PBd_{120}PEO_{89}$	$PBd_{120}PEO_{89}$-NA

Cell Imaging Results of Free Noradrenaline Control

Figure 4.1 shows the cell response to the addition of free NA solution to the cell media (final NA concentration of 1μM). Figure 4.1(A) shows the RASMC region of

study before the addition of free NA and three smaller isolated areas, which were analyzed and compared with the results obtained after the addition of free NA.

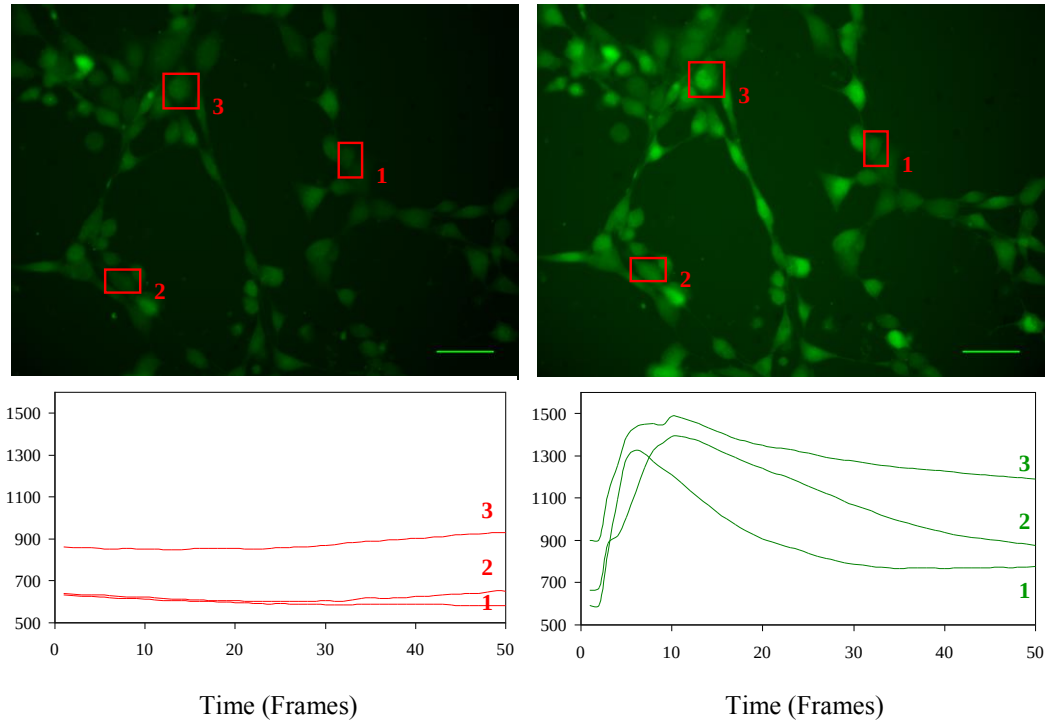

Figure 4.1 Images of RASMC cultures before and after addition of 1μM free NA. (A) Image taken using FITC filter before addition of free NA. (B) Image taken using FITC filter after addition of free NA. The scale bar represents 50 μm in both images. (C) Intensity profile of highlighted areas shown in A. (D) Intensity profile of highlighted areas shown in B.

Figure 4.1(B) shows the same region after the addition of free NA. Figure 4.1(C) shows the intensity profiles of the highlighted areas shown in Figure 4.1(A). During the evaluation period, where no NA was added, the fluorescence intensity stays constant without any substantial variation. Quite the opposite is shown by the intensity profiles presented in Figure 4.1(D) corresponding to Figure 4.1(B). A dramatic increase in the cell's fluorescence intensity was observed due to the presence of free NA molecules.

These images and profiles corroborate that cells react to the presence of NA and provide us with the type of response that should be expected from this cell-drug system.

Cell Imaging Results of Carboxylate-Modified Polystyrene Control Beads

Figure 4.2 shows the cell response to control beads when added to the cell culture. These control beads were exposed to all the reaction steps involved in the covalent linking procedure where NA was used as the primary amine but without the addition of linking agents. For this control beads, no linking reaction was expected to occur and, after the cleaning procedure, microspheres with no modification were obtained. Figure 4.2(A) shows the RASMC region of study before the addition of control beads with three smaller isolated areas. Figure 4.2(B) shows the same region after the addition of control beads. Figure 4.2(C) shows the intensity profiles of the highlighted areas shown in Figure 4.2(A) and it can be observed that during the evaluation period, where no control beads are added, the fluorescence intensity stay almost constant without any substantial variation. Figure 4.2(D) shows the intensity profiles corresponding to Figure 4.2(B) and no significant change in the intensity values with respect to Figure 4.2(C) is observed meaning that there is no NA present to cause cell response. This result support the fact that no NA was linked to the carboxylate beads because of the absence of a linking agent.

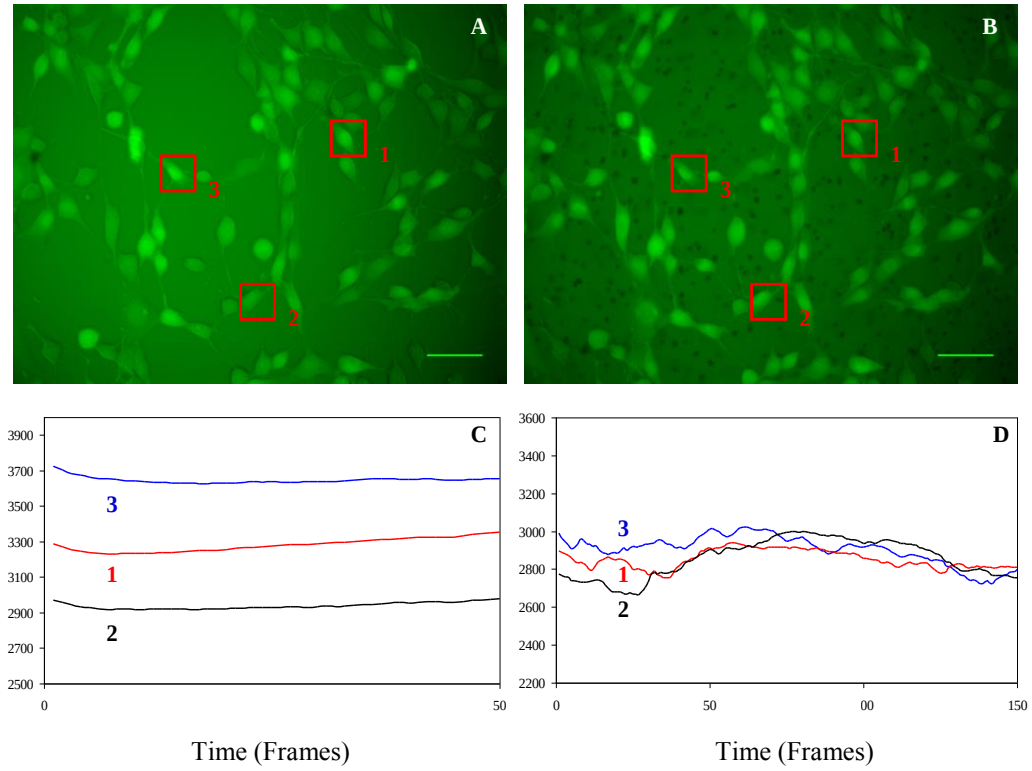

Figure 4.2 Images of RASMC cultures before and after addition of carboxylate-modified polystyrene microspheres control. (A) Fluorescent image taken using FITC filter before addition of control microspheres. (B) Fluorescent image taken using FITC filter after addition of control microspheres. The scale bar represents 50 μm in both images. (C) Intensity profile of highlighted areas shown in A. D. Intensity profile of highlighted areas shown in B.

Cell Imaging Results of Hormone Functionalized Polystyrene Beads

Figure 4.3 shows the cell response to the addition of NA functionalized polystyrene microspheres to the cell culture. These NA functionalized beads are obtained as described in the experimental section. Figure 4.3(A) shows the RASMC region of study before the addition of functionalized beads with three smaller isolated areas. Figure 4.3(B) shows the same region after the addition of functionalized. Figure 4.3(C) plots the intensity profiles of the highlighted areas shown in Figure 4.3(A) and

similar to the previous control experiment, the fluorescence intensity is kept stable during the evaluation time.

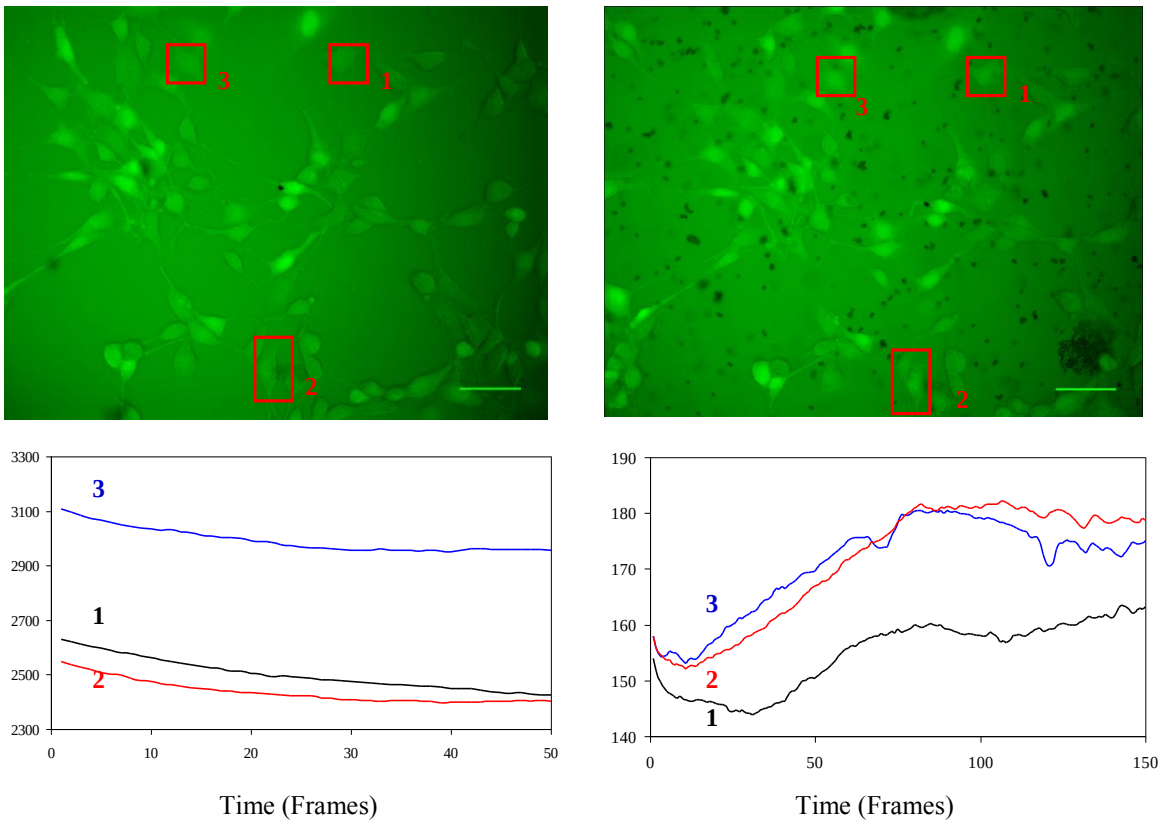

Figure 4.3 Images of RASMC cultures before and after addition of carboxylate-modified polystyrene microspheres covalently linked to NA. (A) Fluorescent image taken using FITC filter before addition of microspheres linked to NA. (B) Fluorescent image taken using FITC filter after addition of microspheres linked to NA. The scale bar represents 50 μm in both images. (C) Intensity profile of highlighted areas shown in A. (D) Intensity profile of highlighted areas shown in B.

Figure 4.3(D) shows the intensity profiles of Figure 4.3(B) and in this case, there is a considerable change in the fluorescence intensity values in contrast to Figure 4.3(C), which means that NA is linked to the carboxylate-modified polystyrene beads through

the EDC/NHS linking chemistry and that the NA carried by these microspheres promotes a cell response. The fluorescence intensity is significantly increased at around frames 20 to 30 (40 seconds to 60 seconds) and increase slopes are observed in the intensity profiles. The smaller intensity increase experienced in this case is attributed to the reduced dose of NA transported by the beads in comparison with the free NA experiment.

Cell Imaging Results of Hormone Functionalized Vesicles and Controls

Figure 4.4 shows two views of a NA functionalized block copolymer vesicle being placed in close contact with the cells surface through micropipette aspiration technique. In the same manner, control vesicle 1 and 2 (previously described in the experimental methods) were evaluated but no significant increase in the cells' fluorescent intensity was observed.

Figure 4.4(A) shows a bright field image where the non-fluorescent vesicle is at the tip of a glass micropipette after applying a small amount of suction while Figure 4.4(B) shows a fluorescent image of the same field of view but neither the vesicle nor the micropipette can be observed. The functionalized vesicles are placed in a rubber chamber that isolate them from the cells until one of them is picked up using a micropipette. In this way, any cell response is ensured due to a single vesicle placed in contact with the cells.

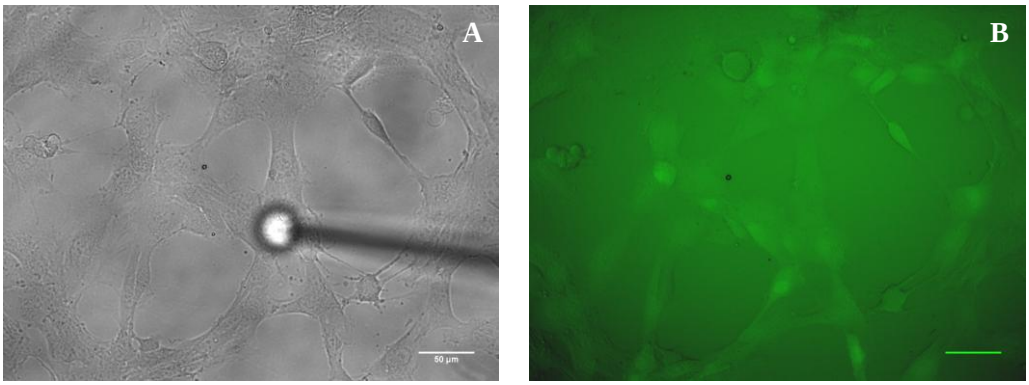

Figure 4.4 Images of a block copolymer vesicle made up with 10% $PBd_{120}PEO_{89}$-NA being placed in close contact with RASMC using micropipette aspiration technique. (A) Bright field image taken using contrast microscopy. (B) Fluorescent image taken using FITC filter. The scale bar represents 50 μm in both images.

Figure 4.5 shows the cell response when a single NA functionalized block copolymer vesicle was placed in contact with the cell's surface. The NA functionalized vesicles were obtained as described in the experimental methods by using 10% of the previously synthesized $PBd_{120}PEO_{89}$-NA block copolymer and 90% of a much shorter diblock copolymer ($PBd_{33}PEO_{20}$). The use of $PBd_{33}PEO_{20}$ allowed the NA functionalized polymer brushes to be more accessible at the vesicle's surface preventing them to be buried and entangled in the vesicle's bilayer region. Figure 4.5(A) shows the RASMC region of study before contact with the functionalized vesicle and three smaller isolated areas. Figure 4.5(B) shows the same region after contact with the functionalized vesicle.

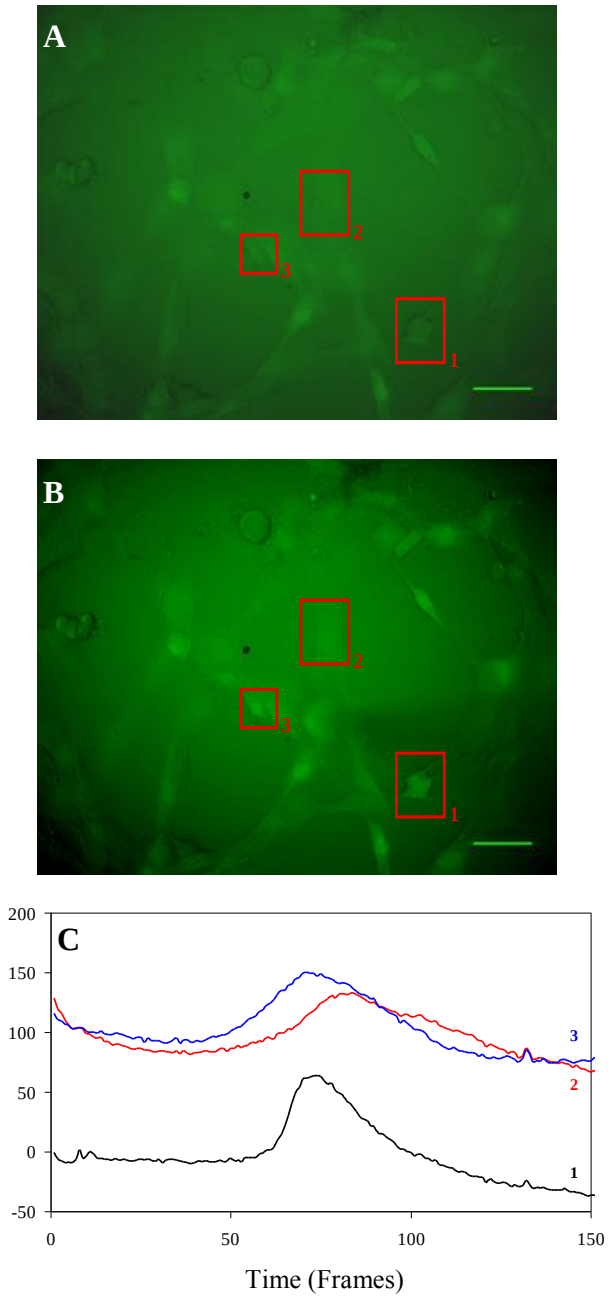

Figure 4.5 Images before and after contact of RASMC culture with a single block copolymer vesicle made with unreacted $PBd_{33}PEO_{20}$ and $PBd_{120}PEO_{89}$-NA mixed in a 9:1 ratio. (A) Fluorescent image taken using FITC filter before putting the cells in contact with a NA functionalized block copolymer vesicle. (B) Fluorescent image taken using FITC filter after putting the cells in contact with a NA functionalized block copolymer vesicle. The scale bar represents 50 μm in both images. (C) Intensity profile of highlighted areas shown in B.

Figure 4.5(C) shows the intensity profiles of the highlighted areas shown in Figure 4.5(B) and a significant increase in the fluorescence intensity values around frame 60 is observed right after the vesicle made contact with the cell surface. After an intensity peak is reached at around frame 75 (150 seconds), the signal decays progressively until the end of the experiment. The difference between the intensity values reached in each case can be explained by the limited NA molecules available at the vesicle's surface producing a low dose response. Also, due to the natural heterogeneity of cells, variant amount of surface receptors existed and different responses can be expected. Signal transmission between exposed and non exposed cells was also observed as well as smooth muscle cell contraction in regions far away from the original stimulus site.

4.8 Conclusions

These series of cell experiments provided us with information about the cell response expected from the RASCM/NA system. The free NA cell experiments showed us what type of cell response was produced when free NA binds to the RASMC surface receptors: An abrupt increase in the fluoresce intensity followed by a progressive intensity decay. The NA functionalized polystyrene microspheres verified that the surface immobilized NA was transported by these beads through simple contact between them and the cell surface.

The use of micropipette aspiration technique provided a different experimental setup that allowed us to study, in a controlled manner, the interaction between a single

NA functionalized polymeric vesicle and the cell surface. The intensity profile recorded during the functionalized vesicle experiment resembled the one of the free NA profile. This profile shape agreement corroborated the hypothesis of NA delivery by the functionalized vesicles. These results reconfirm that NA was transported through these functionalized vesicles and t produced a cell response.

CHAPTER V

REDUCTION-RESPONSIVE FUNCTIONALIZED $PBd_{120}PEO_{89}$ DIBLOCK COPOLYMER VESICLES

5.1 Overview

Due to the increased interest in the high effective of stimuli-responsive drug delivery vehicles, we designed and synthesized a functionalized diblock copolymer that contains a disulfide linkage, which acts as a potential reducible moiety, and a red fluorophore, which simulates a drug molecule. This reduction-responsive diblock copolymer was produced through a simple one-pot two-step reaction in organic solvent by linking cystamine to 5-TAMRA-succinimidyl (product **6**) and then connecting it to carboxylate $PBd_{120}PEO_{89}$ (product **7** or $PBd_{120}PEO_{89}$-cystamine-5-TAMRA) and finally, it was successfully incorporated into a vesicle's bilayer. Exposure to tris(2-carboxyethyl)phosphine hydrochloride (TCEP), which simulates a reductive cytoplasmic environment, caused the disulfide bonds to rupture and to release the drug molecule into solution.

5.2 Introduction

One of the polymersome's applications that has caught great attention is its possibility as a drug delivery system. Various approaches have been carried out to fulfill this aim, and sophisticated designs have been attempted based on the variation and

control of different characteristics of the polymersomes' building blocks. Hammer et al. [63] used of bioresorbable polymeric vesicles of poly(ethylene oxide)-*b*-polycaprolactone where the biodegradability of polycaprolactone was expected to cause a complete *in vivo* degradation of the vesicle to release its enclosed drug. Napoli et al. [103] suggested the use of ABA block copolymers, where polyethylene glycol was used as block A and poly(propylene sulphide), a polymer that contains sulphide moieties, as block B. Here, a mechanism of oxidative destabilization of the vesicles was used to release the contained drug. Sun et al. [104] demonstrated a reduction-responsive biodegradable PEG-SS-PCL micelles and its intracellular drug release capability triggered by a reducing environment. It showed the efficacy and advantages such type of controlled-release in comparison with the traditional drug delivery approach.

Herein, a functionalized block copolymer containing a disulfide moiety was synthesized using a similar amination procedure described in Chapter III. First, the fluorophore 5-TAMRA-succinimidyl was used as a fluorescent marker and linked to a cystamine molecule. No linking agents were required to form the 5-TAMRA-cystamine product due to the presence of an *N*-succinimidyl ester group which greatly enhances the coupling efficiency. Subsequently, an EDC/NHS reaction was performed to link 5-TAMRA-cystamine to the carboxylate $PBd_{120}PEO_{89}$. The final product was a functionalized block copolymer containing the red fluorophore linked to $PBd_{120}PEO_{89}$ with a cystamine molecule in between them (5-TAMRA-cystamine-PEO_{89}-PBd_{120}). Figure 5.1 shows this two-step synthetic pathway.

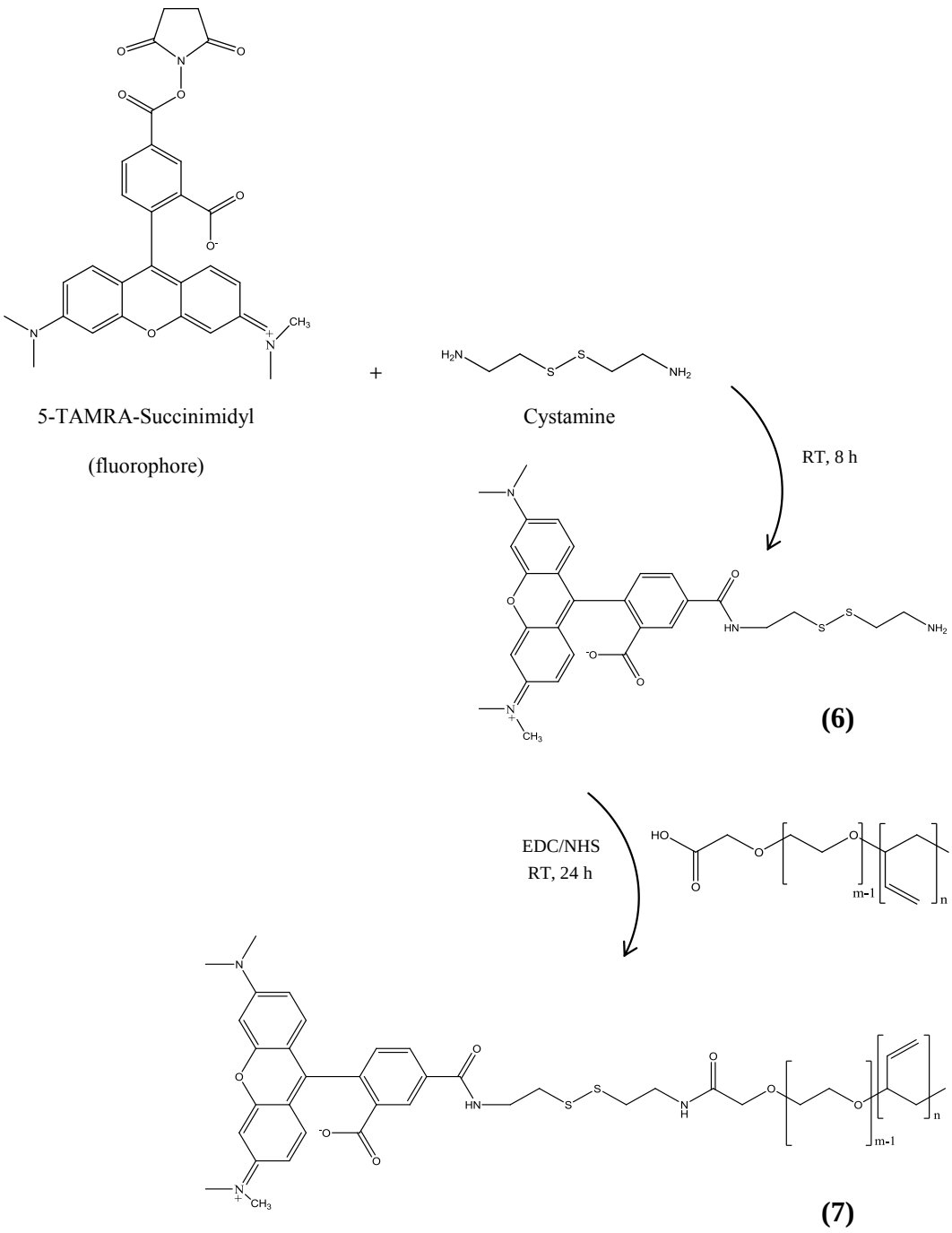

Figure 5.1 Two-step synthesis of functionalized diblock copolymers by covalent coupling of carboxylate $PBd_{120}PEO_{89}$ diblock copolymer to a cystamine and 5-TAMRA-succinimidyl: **(6)** 5-TAMRA-cystamine, after amination reaction between them **(7)** $PBd_{120}PEO_{89}$-cystamine-5-TAMRA, after amination reaction of **(6)** with carboxylate $PBd_{120}PEO_{89}$.

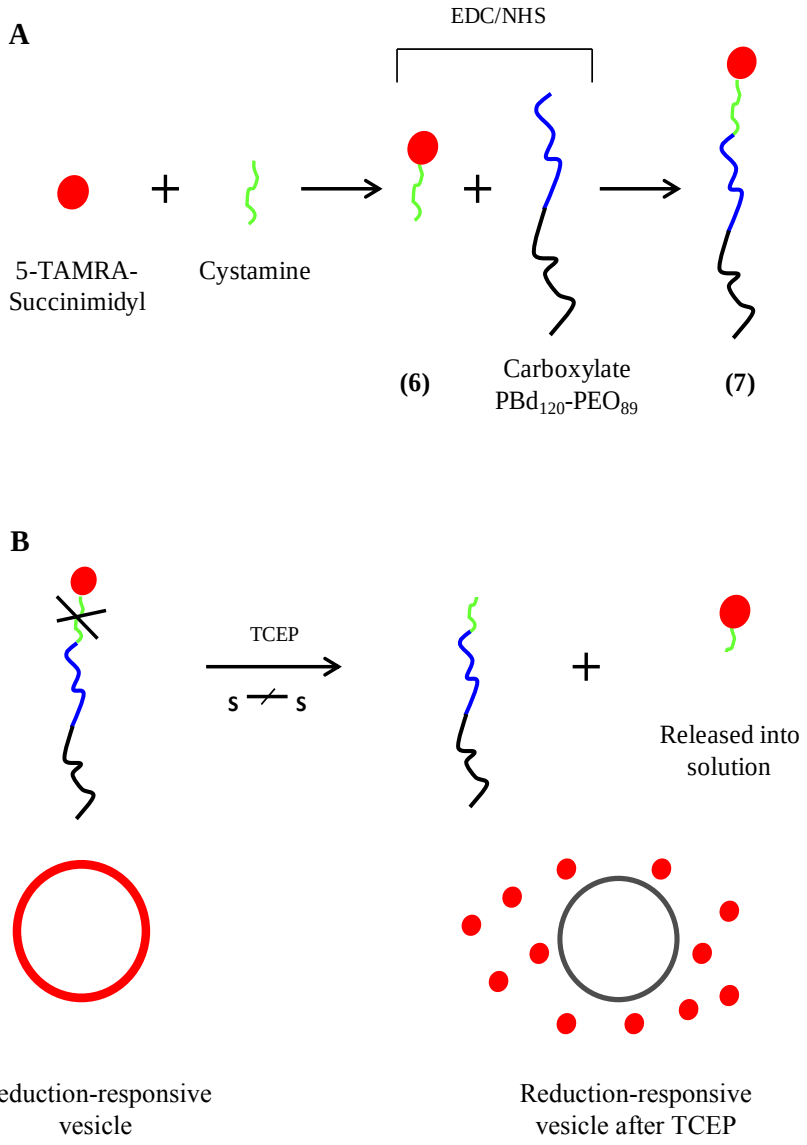

Figure 5.2 Schematic representation of the two-step synthesis of functionalized $PBd_{120}PEO_{89}$-cystamine-5-TAMRA diblock copolymer and its purpose as a reducible surface element once incorporated into a polymersome. (A) Formation of product **7** by covalent coupling of 5-TAMRA-cystamine (**6**) to carboxylate $PBd_{120}PEO_{89}$. (B) Successful incorporation of product **7** into a polymersome and its further exposure to a reducible environment simulated by the presence of TCEP. The change in the polymersome surroundings caused the breakage of disulfide bonds present in product **7** and subsequent release of 5-TAMRA into solution.

Polymersomes containing 10% of this functionalized polymer were formed and imaged under fluorescent microscopy before and after its exposure to a disulfide bond reducing agent such as TCEP. Here, a "selective" approach was attempted in order to stimulate the vesicle system to promote the release of a drug molecule in a reduction environment; the reducing agent was expected to selectively break down the disulfide bonds inside the functionalized polymer and release the attached fluorophore (which simulated a drug molecule) without disturbing the vesicle structure. Figure 5.2 shows a schematic description of the functionalized diblock copolymer synthesis and its reductive application once it was incorporated into vesicles.

5.3 Materials

$PBd_{120}PEO_{89}$ (MW 10400 g/mol) diblock copolymer and sucrose (ACS reagent) ($C_{12}H_{22}O_{11}$, MW 342.3 g/mol) were purchased from Polymer Source Inc. (Canada) and Fisher Scientific (Pittsburgh, PA), respectively. Dichloromethane (anhydrous, 99.9%) (CH_2Cl_2, MW 84.93 g/mol), chloroform (99.8+% for analysis ACS, stabilized with ethanol) ($CHCl_3$, MW 119.38 g/mol) and methanol (99.8+% for analysis ACS) (MeOH, MW 32.04 g/mol) were purchased from Acros Organics (Morris Plains, NJ). Tetrahydrofuran (≥ 99.0% ACS reagent) (THF, MW 72.11 g/mol), cystamine dihydrochloride (MW 225.20 g/mol) and tris(2-carboxyethyl)phosphine hydrochloride (TCEP, MW 286.65 g/mol) were purchased from Sigma-Aldrich (St. Louis, MO). 5-Carboxy-tetramethylrhodamine *N*-succinimidyl ester (5-TAMRA-succinimidyl, MW 527.52 g/mol) was purchased from Fluka (Switzerland). 1-Ethyl-3-

[3-dimethylaminopropyl]carbodiimide hydrochloride (EDC, MW 191.70) and *N*-Hydroxysuccinimide (NHS, MW 115.09 g/mol) were purchased from Pierce (Rockford, IL). Regenerated cellulose dialysis tubing kit (MWCO 8000 g/mol) was purchased from Spectra/Por®Biotech and, the previously synthesized carboxylate PBd_{120}-PEO_{89} diblock copolymer.

5.4 Experimental Methods

Diblock Copolymer Characterization

IR Spectroscopy. IR spectra of neat liquids were performed using a Bruker FT-IR TENSOR™ spectrometer (Billerica, MA) equipped with OPUS™ measurement software. Potassium bromide salt plates (McCarthy Scientific Co., Fallbrook, CA) and CH_2Cl_2, or $CHCl_3$, were used to evaluate the polymer samples.

Vesicle Solution Characterization

Cross-Polarizing Fluorescent Microscopy. Vesicle solutions were imaged using the temporary closed sample chamber described in Chapter III. Phase contrast images of polymersomes were taken by a Carl Zeiss Axiovert 200M inverted microscope with 100 W HBO Mercury vapor lamp coupled to a Zeiss AxioCam MRm camera and a 20X objective (numerical aperture of 0.5). Fluorescent microscope images were obtained using a rhodamine band-pass filter with an excitation wavelength of 545 nm (bandwidth of 25 nm) and an emission wavelength of 605 nm (bandwidth of 70 nm). To facilitate comparison of samples to controls, all images were taken sequentially using the same

instrumental parameters and the recorded images were processed and analyzed identically with the program ImageJ.

Treatment of Functionalized Vesicles with TCEP

10 μL of an equimolar solution of TCEP was added to the vesicle solution to be observed by fluorescent microscopy. The vesicle solution containing TCEP was gently stirred and allowed to react for 30 minutes before taking the images.

5.5 Synthesis of $PBd_{120}PEO_{89}$-cystamine-5-TAMRA

The reactions were conducted under an argon atmosphere and stirred using a Teflon-covered stir bar. A 5 mL reaction flask was charged with 1 mL of 1:1 MeOH:$CHCl_3$ solution, $10x10^{-3}$ mmol of cystamine dihydrochloride and $1x10^{-3}$ mmol of 5-TAMRA-succinimidyl. The mixture was allowed to react for 8 hours at room temperature under constant magnetic stirring (900 rpm). After completion, 5-TAMRA-succinimidyl is linked to cystamine at one of its ends only since it was present in excess amount. 1 mL ($1x10^{-3}$ mmol) of 1:1 MeOH:$CHCl_3$ solution of carboxylate PEO_{89}-PBd_{120}, $10x10^{-3}$ mmol of EDC and $10x10^{-3}$ mmol of NHS were added to the reaction flask and allowed to react for 24 hours at room temperature under constant magnetic stirring (900 rpm). Extra doses of EDC and NHS were added every two hours to increase the amount of cystamine-5-TAMRA linked to carboxylate groups.

Synthesis of (6)

5-carboxy-tetramethylrhodamine N-succinimidyl ester (1.54 mg, 2.92×10^{-3} mmol) and cystamine dihydrochloride (3.29 mg, 14.62×10^{-3} mmol) were reacted in methanol/chloroform as described above. Product **6** was obtained but not purified and used to continue with the synthesis of **7**.

Synthesis of (7)

Carboxylate PBd_{120}-PEO_{89} (30.40 mg, 2.92×10^{-3} mmol), EDC (5.60 mg, 29.23×10^{-3} mmol), NHS (1.68 mg, 14.62×10^{-3} mmol) and product **6** were reacted in methanol/chloroform as described above. In this manner, product **7** (22.80 mg, 75% yield) was obtained. IR (ν): 1695 (C=O) cm^{-1}, 1539 (N-H bend) cm^{-1}.

Synthesis of Diblock Copolymer Controls

The modified diblock copolymers used in controls were prepared using different components and were labeled as follow: Control 1: when cystamine, 5-TAMRA-succinimidyl, $PBd_{120}PEO_{89}$, EDC and NHS were combined; control 2: when cystamine, 5-TAMRA-succinimidyl and carboxylate $PBd_{120}PEO_{89}$ were combined; sample: when cystamine, 5-TAMRA-succinimidyl, carboxylate $PBd_{120}PEO_{89}$, EDC and NHS were combined (Figure 5.3).

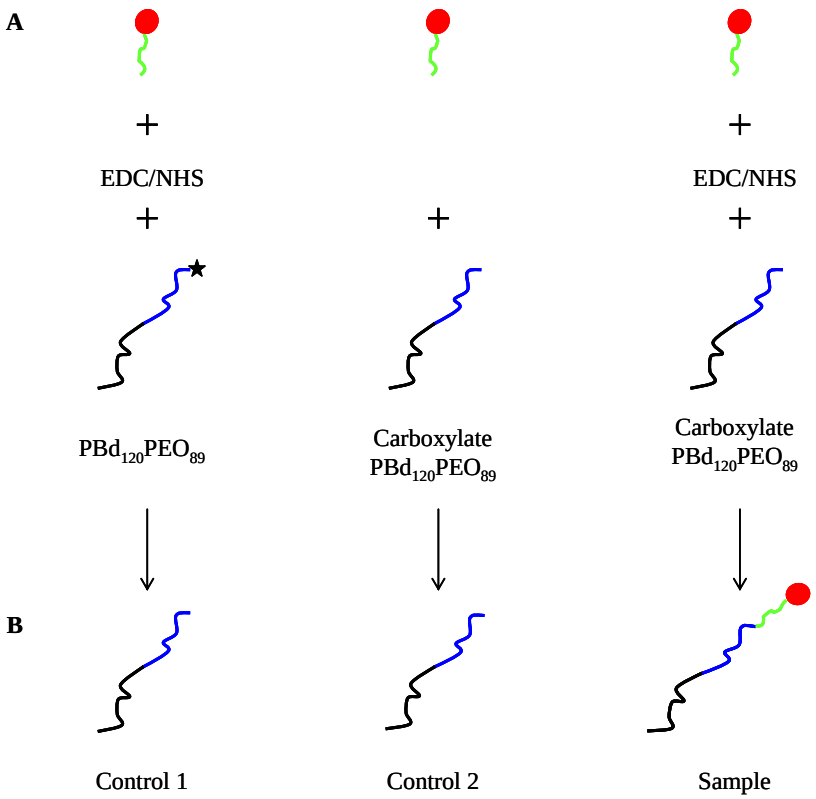

Figure 5.3 Schematic representations of controls and sample synthesis of functionalized $PBd_{120}PEO_{89}$-cystamine-5-TAMRA diblock copolymer. (A) Control 1: cystamine-5-TAMRA, EDC, NHS and unmodified $PBd_{120}PEO_{89}$; control 2: cystamine-5-TAMRA and carboxylate $PBd_{120}PEO_{89}$ and, sample: cystamine-5-TAMRA, EDC, NHS and carboxylate $PBd_{120}PEO_{89}$. (B) Final control and sample products incorporated into a polymersome.

Functionalized Polymer Cleaning Procedure

The desired product, was redisolved in 2 mL of a 1:1 MeOH:$CHCl_3$ solution and cleaned using regenerated cellulose dialysis tubing (MWCO 8000 g/mol). The sample was dialyzed for 2 hours at room temperature against 600 mL (300 times the volume of the sample) of 1:1 MeOH:$CHCl_3$ solution, the dialysis buffer was changed and the sample dialyzed for another 2 hours. Finally, the dialysis buffer was changed for the second time and the sample dialyzed overnight.

5.6 Vesicle Solution Preparation

A polymer film containing 100 μg of the desired block copolymer or block copolymer mixture was formed by evaporation (8 hours) at the bottom of a 5 mL glass scintillation vial. Polymersomes were formed by rehydration of this polymer film during 24 hours at 60ºC with 2 mL of 300 mOsm/kg sucrose solution. A vesicle solution of the following mixture composition was formed: 10% w/w of $PBd_{120}PEO_{89}$-cystamine-5-TAMRA and 90% w/w of unmodified $PBd_{120}PEO_{89}$. The final block copolymer concentration in a vesicle solution of 2 mL is 4.8 μM.

Vesicle Solution Controls

Two vesicle solutions of controls were prepared by combining in a 9:1 ratio the unreacted $PBd_{120}PEO_{89}$ and the functionalized diblock copolymer control 1 or control 2.

5.7 Results and Discussion

IR Results from Amination Reaction

Figure 5.4 shows the overlay IR spectra of the carboxylate $PBd_{120}PEO_{89}$ (top) and $PBd_{120}PEO_{89}$-cystamine-5-TAMRA-succinimidyl (bottom). The presence of a carbonyl stretch peak at around 1695 cm^{-1} and N-H bend peak at 1456 cm^{-1} demonstrates the formation of a peptide linkage between the primary amines (cystamine and 5-TAMRA-succinimidyl) and the carboxylate $PBd_{120}PEO_{89}$.

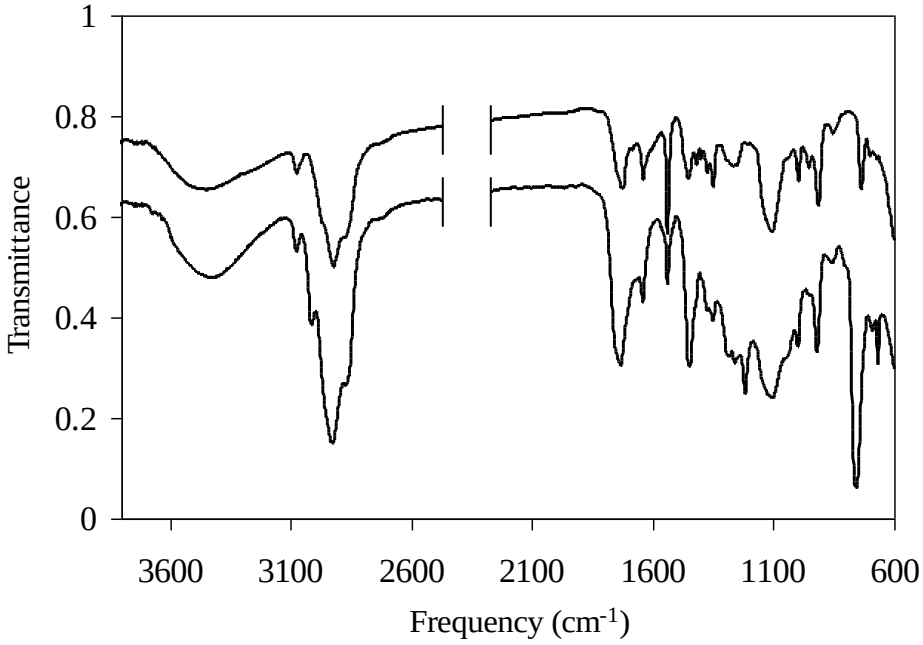

Figure 5.4 Comparison between the IR spectra of the unmodified carboxylate $PBd_{120}PEO_{89}$ (top) and the covalent coupling reaction product, $PBd_{120}PEO_{89}$-cystamine-5-TAMRA (bottom).

Imaging Results of Functionalized $PBd_{120}PEO_{89}$-cystamine-5-TAMRA Vesicles

Figure 5.5 and Figure 5.6 show three vesicle samples obtained by using unmodified $PBd_{120}PEO_{89}$ and $PBd_{120}PEO_{89}$-cystamine-5-TAMRA block copolymer previously synthesized in a 9:1 ratio. Figure 5.5(A) shows red fluorescent vesicles which confirm that 5-TAMRA-succinimidyl is linked to the carboxylate PEO_{89}-PBd_{120} through the proposed amination reaction. Figure 5.5(B) shows their respective intensity profiles with an average peak intensity of 192.7 units (standard deviation of 30.6 units).

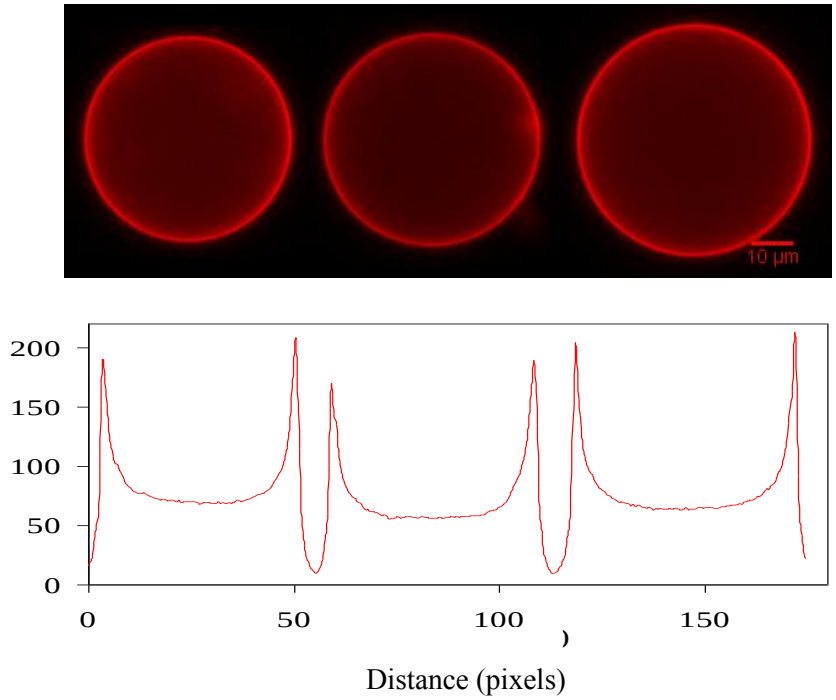

Figure 5.5 Images of fluorescent block copolymer vesicles made with unreacted $PBd_{120}PEO_{89}$ and $PBd_{120}PEO_{89}$-cystamine-5-TAMRA mixed in a 9:1 ratio before exposure to TCEP. (A) Fluorescent images taken using a rhodamine filter. (B) Intensity profiles corresponding to each fluorescent vesicle shown in A.

Table 5.1 Intensity profile values of $PBd_{120}PEO_{89}$-cystamine-5-TAMRA functionalized vesicles before and after exposure to TCEP. Average values of bilayer peak 1 and 2 of five different samples are shown and compared and in all cases, a decrease in the fluorescence intensity was registered after exposure to TCEP.

	Functionalized Vesicle (Intensity units)			**Functionalized Vesicle After Exposure to TCEP (Intensity units)**		
	Peak 1	**Peak 2**	**Average**	**Peak 1**	**Peak 2**	**Average**
Trial 1	190.2	207.5	**198.9**	72.9	92.8	**82.8**
Trial 2	170.1	189.4	**179.7**	103.0	102.5	**102.8**
Trial 3	203.5	212.8	**208.2**	120.5	139.6	**130.1**
Trial 4	225.0	232.3	**228.6**	148.5	128.9	**138.7**
Trial 5	146.7	149.0	**147.8**	82.0	89.7	**85.9**
StDev			**30.6**			**25.4**

Figure 5.6(A) shows three different vesicle samples after addition of TCEP to the vesicle solution while Figure 5.6(B) shows their respective intensity profiles with an average peak intensity of 108.0 units (standard deviation of 25.4 units). Individual vesicles exhibit lower fluorescence intensity after exposing the vesicle solution to TCEP. Tables 5.1 and 5.2 show the average intensity profile values of bilayer peaks 1 and 2 and the fluorescent intensity percentage decrease of five functionalized vesicles before and after addition of TCEP.

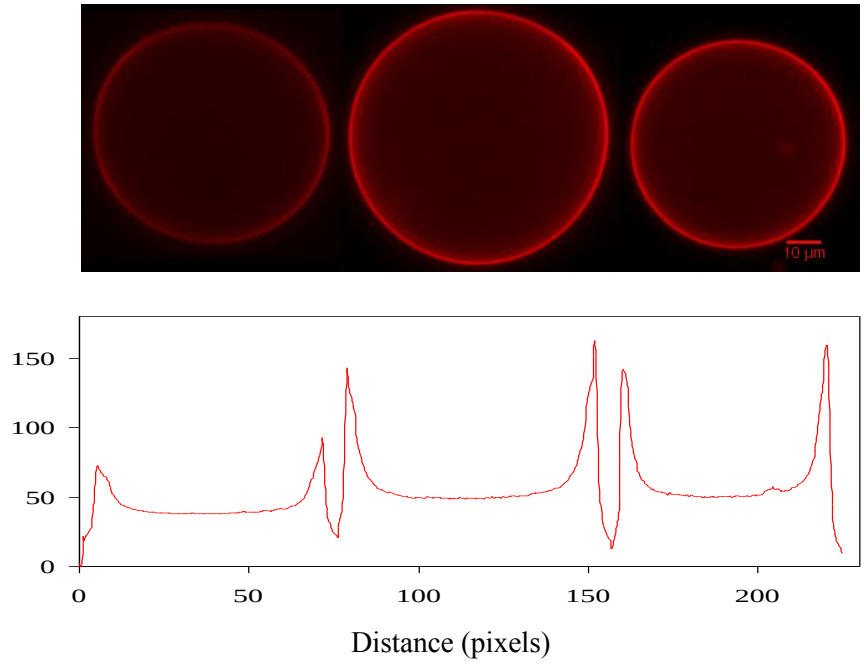

Figure 5.6 Images of fluorescent block copolymer vesicles made with unreacted $PBd_{120}PEO_{89}$ and $PBd_{120}PEO_{89}$-cystamine-5-TAMRA mixed in a 9:1 ratio after exposure to TCEP. (A) Fluorescent images taken using a rhodamine filter. (B) Intensity profiles corresponding to each fluorescent vesicle shown in A.

Vesicles formed in a 9:1 ratio with unreacted $PBd_{120}PEO_{89}$ and $PBd_{120}PEO_{89}$-cystamine-5-TAMRA polymers show a difference in the fluorescence intensities before and after treating the vesicle solutions with TCEP. A 44% decrease in fluorescence intensity was recorded after a change in the polymersome environment. This difference is attributed to the selective reduction of disulfide bonds present in the $PBd_{120}PEO_{89}$-cystamine-5-TAMRA block copolymer. When the disulfide bonds are broken, 5-TAMRA is released and lower fluorescent intensity was observed in the vesicle's bilayer. However, it is not determined if the fluorophore was released into the aqueous solution or if it was partially redisolved into the vesicle's bilayer.

Table 5.2 Average intensity profile values of $PBd_{120}PEO_{89}$-cystamine-5-TAMRA functionalized vesicles before and after exposure to TCEP of 5 different samples. A 44% decrease in fluorescence intensity was recorded after a change in the polymersome environment was produced.

	Functionalized Vesicle (Intensity units)	**Functionalized Vesicle After Exposure to TCEP (Intensity units)**	**% Intensity decrease**
Trial 1	198.9	82.8	58.3
Trial 2	179.7	102.8	42.8
Trial 3	208.2	130.1	37.5
Trial 4	228.6	138.7	39.4
Trial 5	147.8	85.9	41.9
Average	**192.7**	**108.0**	**43.9**
StDev	**30.6**	**25.4**	**8.3**

5.8 Conclusions

The functionalized reductive-responsive diblock copolymer $PBd_{120}PEO_{89}$-cystamine-5-TAMRA was synthesized using a one-pot two-step reaction and has been

incorporated into polymersomes with a 10% amount. A fluorophore was attached at the end of the diblock for imaging purposes but virtually any suitable drug molecule can replace it and be carried by a polymersome.

The reductive character of the diblock was given by the presence of a disulfide linkage between the PEO block and the fluorophore molecule. When $PBd_{120}PEO_{89}$-cystamine-5-TAMRA functionalized polymersomes were formed, the reductive character of this new diblock was preserved in the vesicle's configuration.

Functionalized vesicles were exposed to a reducible environment by the addition of TCEP. The diblock copolymer disulfide bonds were selectively reduced and the fluorophore 5-TAMRA was released into solution. Fluorescent microscopy showed that the vesicle's bilayer fluorescent intensity decreased by 44 % and, we can infer from this result that about 44% of the attached 5-TAMRA was released.

These stimuli-responsive vesicles can be used as reliable drug delivery carriers that at the encounter of the cell's cytoplasm, which is characterized as a reductive environment, will break the susceptible bonds and release the transported drug molecules.

CHAPTER VI

CONCLUSIONS AND FUTURE DIRECTIONS

6.1 Conclusions

We proved that the primary alcohol end group of the $PBd_{120}PEO_{89}$ diblock copolymer can be chemically modified and effectively combined with unmodified $PBd_{120}PEO_{89}$ to form stable functionalized polymeric vesicles. The free hydroxyl terminal group of the PEO block was first oxidized to its corresponding carboxylic acid through a regioselective one-pot two-phase oxidation reaction while other oxidizable groups present in the diblock copolymer backbone remained unaffected. Subsequently, three primary amines (two fluorophores and a hormone molecule) were able to be covalently attached to the previously synthesized carboxylate diblock through a modified coupling reaction performed in organic phase (Chapter III).

Polymersomes containing 90% of the unmodified $PBd_{120}PEO_{89}$ diblock copolymers and 10% of one of the modified diblock copolymers ($PBd_{120}PEO_{89}$-6AF, $PBd_{120}PEO_{89}$-COU and $PBd_{120}PEO_{89}$-NA) has been prepared. In addition, the two fluorescently modified diblock copolymers ($PBd_{120}PEO_{89}$-6AF and $PBd_{120}PEO_{89}$-COU) have been properly integrated into the same vesicle, and surface density control of the two fluorophores was achieved suggesting that these drug delivery prototypes can be tailored (Chapter IV).

The measured CAC values of vesicle solutions containing a mixture of carboxylate $PBd_{120}PEO_{89}$ and unmodified $PBd_{120}PEO_{89}$ were found to increase as the carboxylate $PBd_{120}PEO_{89}$ content increased, in the meantime the average vesicle size decreased. This observation suggests that the carboxylic acid group lowered the polymer's ability to be incorporated into a polymersome when present in concentrations higher than 80 percent.

In Chapter IV, RASMC essays reveal that hormone functionalized polymeric vesicles (containing NA) were able to deliver the hormone molecules that are carried at the vesicle's surface. It was confirmed by the increase in the cells' fluorescent intensity after placing a functionalized vesicle in close contact with the cell's surface.

As discussed in Chapter V, a rhodamine functionalized diblock copolymer containing a disulfide linkage between the PEO block and the fluorophore (PBd_{120}-PEO_{89}-cystamine-5-TAMRA) has been synthesized. This reducible functionalized polymer, specifically designed to be susceptible to disulfide bond cleavage when exposed to a reducing environment, was effectively integrated into a polymersome. The disulfide moiety has show to be selectively reduced when exposed to a change in the surrounding conditions promoted by the addition of the reducing agent TCEP. The fluorophore was released into solution indicating that these polymersomes can be used as stimuli responsive drug delivery carriers.

6.2 Future Directions

For future studies, the diblock copolymer used may be substituted by a biodegradable one and apply to it the synthesis explored during this research. Functionalized biodegradable polymersomes, their cell internalization and degradation time can be systematically investigated in order to elucidate their response mechanism.

Hormone functionalized vesicles might be further studied to better understand the cell's response, drug internalization, drug release profiles and long distance intracellular communication. Also, stimuli-responsive functionalized polymersomes vulnerable to reducible atmospheres might be evaluated in contact with RASMC cultures to establish the reductive strength of the cytoplasmic environment over the disulfide moieties employed.

Vesicle solutions containing 10% w/w $PBd_{120}PEO_{89}$-cystamine-5-TAMRA reducible functionalized diblock copolymer and 90% w/w $PBd_{33}PEO_{20}$ (a shorter diblock, MW 2700 g/mol) might be formed and evaluated in order to enhance the availability of the functionalized polymer to TCEP by preventing polymer entanglements.

A reductive destabilization mechanism involving a phase transition from vesicle to micelle may also be investigated. A PEO-PBd diblock copolymer linked to a second PEO block by a cystamine molecule can be synthesized and polymersomes containing this PEO-PBd-cystamine-PEO amphiphillic polymer might be formed. The reduction of the disulfide moiety present in cystamine by TCEP may induce a morphological change from highly stable vesicles to micelles (Figure 6.1). This change in surface topology, in

response to a change in the environment character, may be useful to create a stimuli responsive drug delivery vehicle.

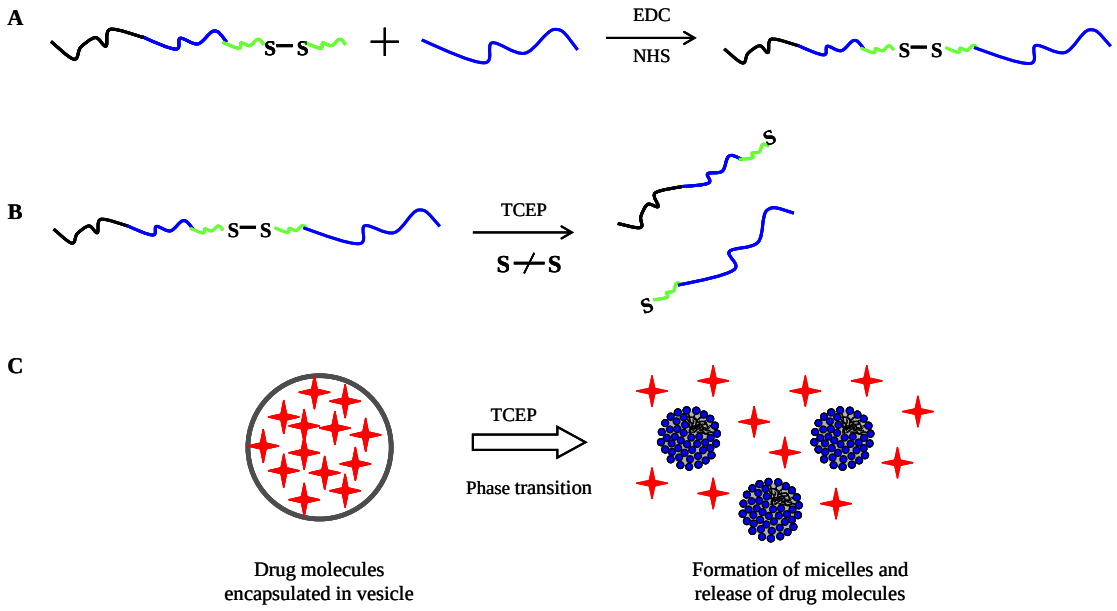

Figure 6.1 Schematic representation of the two-step synthesis of functionalized PBd_mPEO_n-cystamine-$PEO_{(m-n)}$ block copolymer and its possible function as a stimuli responsive reducible component. (A) Formation functionalized diblock by covalent coupling reaction. (B) Exposure of functionalized polymersome to reducing agent might cause breakage of disulfide bonds. (C) Functionalized polymersome encapsulating drug molecules (represented by red stars) may experience a morphological change from vesicle to micelles causing control release of transported molecules when exposed to a reducing environment.

REFERENCES

1. Lipowsky R, Sackmann E, Hoff AJ. Handbook of biological physics. Leiden; Elsevier; 1995.

2. Lipowsky R. The conformation of membranes. Nature. 1991;349:475-81.

3. Lipowsky R, Sackmann E. Structure and dynamics of membranes. Oxford; Elsevier; 1995.

4. Lipowsky R. The morphology of lipid membranes. Current Opinion in Structural Biology. 1995;5:531-40.

5. Lasic DD. The mechanism of vesicle formation. Biochemical Journal. 1988;256:1-11.

6. Bangham AD. Lipid bilayers and biomembranes. Annual Review of Biochemistry. 2003;41:753-76.

7. Deuling HJ, Helfrich W. The curvature elasticity of fluid membranes: A catalogue of vesicle shapes. Journal de Physique. 1976;37:1335-45.

8. Lasic D. Liposomes. American Scientist. 1992;80:20-31.

9. Lasic DD. Formation of membranes. Nature. 1991;351:613-.

10. Sackmann E, Engelhardt J, Fricke K, Gaub H. On dynamic molecular and elastic properties of lipid bilayers and biological membranes. Colloids and Surfaces. 1984;10:321-35.

11. Safran SA, Pincus P, Andelman D. Theory of spontaneous vesicle formation in surfactant mixtures. Science. 1990;248:354-6.

12. Segota S, Tezak D. Spontaneous formation of vesicles. Advances in Colloid and Interface Science. 2006;121:51-75.

13. Singer SJ, Nicolson GL. Fluid mosaic model of structure of cell-membranes. Science. 1972;175:720-&.

14. Szoka F, Papahadjopoulos D. Comparative properties and methods of preparation of lipid vesicles (liposomes). Annual Review of Biophysics and Bioengineering. 1980;9:42.

15. Bangham AD, Horne RW. Negative staining of phospholipids + their structural modification by-surface active agents as observed in electron microscope. Journal of Molecular Biology. 1964;8:660-&.

16. Gobley M. Examen comparatif du jaune d'oeufe et de al matiere cerebrale. J Pharm Chim. 1847;17:409.

17. Hicks M, Gebicki JM. Microscopic studies of fatty acid vesicles. Chemistry and Physics of Lipids. 1977;20:243-52.

18. Gebicki JM, Hicks M. Preparation and properties of vesicles enclosed by fatty acid membranes. Chemistry and Physics of Lipids. 1976;16:142-60.

19. Colley CM, Ryman BE. The liposome: from membrane model to therapeutic agent. Trends in Biochemical Sciences. 1976;1:203-5.

20. Zhdanov VP, Kasemo B. Simulation of diffusion of vesicles at a solid-liquid interface. Langmuir. 2000;16:4416-9.

21. Cohen BE. Concentration-dependence and time-dependence of amphotericin-B induced permeability changes across ergosterol-containing liposomes. Biochimica Et Biophysica Acta. 1986;857:117-22.

22. Gouaux E, MacKinnon R. Principles of selective ion transport in channels and pumps. Science. 2005;310:1461-5.

23. Weber G, Jayaram HN, Pillwein K, Natsumeda Y, Reardon MA, Zhen YS. Salvage pathways as targets of chemotherapy. Advances in Enzyme Regulation. 1987;26:335-52.

24. Presant CA, Multhauf P, Metter G. Reversal of cancer chemotherapeutic resistance by amphotericin B-a broad phase I-Ii pilot-study. European Journal of Cancer & Clinical Oncology. 1987;23:683-7.

25. Gregoriadis G, Swain CP, Wills EJ, Tavill AS. Drug-carrier potential of liposomes in cancer chemotherapy. The Lancet. 1974;303:1313-6.

26. Grant CWM, Hamilton KS, Hamilton KD, Barber KR. Physical biochemistry of a liposomal amphotericin-B mixture used for patient treatment. Biochimica Et Biophysica Acta. 1989;984:11-20.

27. Honeywell-Nguyen PL, Bouwstra JA. Vesicles as a tool for transdermal and dermal delivery. Drug Discovery Today: Technologies. 2005;2:67-74.

28. Lasic DD. Mixed micelles in drug delivery. Nature. 1992;355:279-80.

29. Powderly WG, Kobayashi GS, Herzig GP, Medoff G. Amphotericin B-resistant yeast infection in severely immunocompromised patients. American Journal of Medicine. 1988;84:826-32.

30. Sculier JP, Coune A, Meunier F, Brassinne C, Laduron C, Hollaert C, et al. Pilot-study of amphotericin-B entrapped in sonicated liposomes in cancer-patients with fungal-infections. European Journal of Cancer & Clinical Oncology. 1988;24:527-38.

31. Washington C, Taylor SJ, Davis SS. The structure of colloidal formulations of amphotericin-B. International Journal of Pharmaceutics. 1988;46:25-30.

32. McDermott MM, Kerwin DR, Liu K, Martin GJ, O'Brien E, Kaplan H, et al. Prevalence and significance of unrecognized lower extremity peripheral arterial disease in general medicine practice. Journal of General Internal Medicine. 2001;16:384-90.

33. Liu SC, O'Brien DF. Stable polymeric nanoballoons: lyophilization and rehydration of cross-linked liposomes. Journal of the American Chemical Society. 2002;124:6037-42.

34. Ringsdorf H, Schlarb B, Venzmer J. Molecular architecture and function of polymeric oriented systems - Models for the study of organization, surface recognition, and dynamics of biomembranes. Angewandte Chemie-International Edition in English. 1988;27:113-58.

35. Volodkin DV, Ball V, Voegel J-C, Mˆhwald H, Dimova R, Marchi-Artzner V. Control of the interaction between membranes or vesicles: Adhesion, fusion and release of dyes. Colloids and Surfaces A: Physicochemical and Engineering Aspects. 2007;303:89-96.

36. Lipowsky R. Statistical physics of flexible membranes. Physica A: Statistical Mechanics and its Applications. 1993;194:114-27.

37. McMahon HT, Gallop JL. Membrane curvature and mechanisms of dynamic cell membrane remodelling. Nature. 2005;438:590-6.

38. Lasic DD. Giant Vesicles: A Historical Introduction. In: Perspectives in Supramolecular Chemistry; Luisi PL, Walde P. Zurich, editors. John Wiley & Sons, Ltd; 2007, p. 11-24.

39. Lee JCM, Bermudez H, Discher BM, Sheehan MA, Won YY, Bates FS, et al. Preparation, stability, and in vitro performance of vesicles made with diblock copolymers. Biotechnology and Bioengineering. 2001;73:135-45.

40. Israelachvili JN. Intermolecular and surface forces. 2nd ed. London: Academic Press; 1992.

41. Kabanov AV, Bronich TK, Kabanov VA, Yu K, Eisenberg A. Spontaneous formation of vesicles from complexes of block ionomers and surfactants. Journal of the American Chemical Society. 1998;120:9941-2.

42. Kaler EW, Murthy AK, Rodriguez BE, Zasadzinski JAN. Spontaneous vesicle formation in aqueous mixtures of single-tailed surfactants. Science. 1989;245:1371-4.

43. Evans DF, Wennerstro\m HA. The colloidal domain : where physics, chemistry, biology, and technology meet. 2nd ed. New York: Wiley-VCH; 1999.

44. Hammer DA, Discher DE. Synthetic cells-self-assembling polymer membranes and bioadhesive colloids. Annual Review of Materials Research. 2001;31:387-404.

45. Discher DE, Eisenberg A. Polymer vesicles. Science. 2002;297:967-73.

46. Crespo JS, Lecommandoux S, Borsali R, Klok HA, Soldi V. Small-angle neutron scattering from diblock copolymer poly(styrene-d(8))-b-poly(gamma-benzyl L-glutamate) solutions: Rod-coil to coil-coil transition. Macromolecules. 2003;36:1253-6.

47. Discher BM, Won YY, Ege DS, Lee JCM, Bates FS, Discher DE, et al. Polymersomes: Tough vesicles made from diblock copolymers. Science. 1999;284:1143-6.

48. Bermudez H, Brannan AK, Hammer DA, Bates FS, Discher DE. Molecular weight dependence of polymersome membrane structure, elasticity, and stability. Macromolecules. 2002;35:8203-8.

49. Bermudez H, Hammer DA, Discher DE. Effect of bilayer thickness on membrane bending rigidity. Langmuir. 2004;20:540-3.

50. Evans E, Needham D. Physical-properties of surfactant bilayer-membranes - Thermal transitions, elasticity, rigidity, cohesion, and colloidal interactions. Journal of Physical Chemistry. 1987;91:4219-28.

51. Lin JJ, Silas JA, Bermudez H, Milam VT, Bates FS, Hammer DA. The effect of polymer chain length and surface density on the adhesiveness of functionalized polymersomes. Langmuir. 2004;20:5493-500.

52. Luo LB, Eisenberg A. Thermodynamic stabilization mechanism of block copolymer vesicles. Journal of the American Chemical Society. 2001;123:1012-3.

53. Aranda-Espinoza H, Bermudez H, Bates FS, Discher DE. Electromechanical limits of polymersomes. Physical Review Letters. 2001;8720.

54. Shen HW, Eisenberg A. Morphological phase diagram for a ternary system of block copolymer PS310-b-PAA(52)/dioxane/H2O. Journal of Physical Chemistry B. 1999;103:9473-87.

55. Discher BM, Hammer DA, Bates FS, Discher DE. Polymer vesicles in various media. Current Opinion in Colloid & Interface Science. 2000;5:125-31.

56. Soo PL, Eisenberg A. Preparation of block copolymer vesicles in solution. Journal of Polymer Science Part B: Polymer Physics. 2004;42:923-38.

57. Hillmyer MA, Bates FS. Synthesis and characterization of model polyalkane-poly(ethylene oxide) block copolymers. Macromolecules. 1996;29:6994-7002.

58. Batycky RP, Hanes J, Langer R, Edwards DA. A theoretical model of erosion and macromolecular drug release from biodegrading microspheres. Journal of Pharmaceutical Sciences. 1997;86:1464-77.

59. Borner HG, Schlaad H. Bioinspired functional block copolymers. Soft Matter. 2007;3:394-408.

60. Hagan SA, Coombes AGA, Garnett MC, Dunn SE, Davis MC, Illum L, et al. Polylactide-poly(ethylene glycol) copolymers as drug delivery systems. 1. Characterization of water dispersible micelle-forming systems. Langmuir. 1996;12:2153-61.

61. Wootton DM, Ku DN. Fluid mechanics of vascular systems, diseases, and thrombosis. Annual Review of Biomedical Engineering. 1999;1:299-329.

62. Yamaoka T, Tabata Y, Ikada Y. Distribution and tissue uptake of poly(ethylene glycol) with different molecular-weights after intravenous administration to mice. Journal of Pharmaceutical Sciences. 1994;83:601-6.

63. Ghoroghchian PP, Li GZ, Levine DH, Davis KP, Bates FS, Hammer DA, et al. Bioresorbable vesicles formed through spontaneous self-assembly of amphiphilic poly(ethylene oxide)-block-polycaprolactone. Macromolecules. 2006;39:1673-5.

64. Lomas H, Canton I, MacNeil S, Du J, Armes SP, Ryan AJ, et al. Biomimetic pH sensitive polymersomes for efficient DNA encapsulation and delivery. Advanced Materials. 2007;19:4238-43.

65. Checot F, Lecommandoux S, Klok HA, Gnanou Y. From supramolecular polymersomes to stimuli-responsive nano-capsules based on poly(diene-b-peptide) diblock copolymers. European Physical Journal E. 2003;10:25-35.

66. Ghoroghchian PP, Frail PR, Susumu K, Blessington D, Brannan AK, Bates FS, et al. Near-infrared-emissive polymersomes: Self-assembled soft matter for in vivo optical imaging. Proceedings of the National Academy of Sciences of the United States of America. 2005;102:2922-7.

67. Zandstra PW, Nagy A. Stem cell bioengineering. Annual Review of Biomedical Engineering. 2001;3:275-305.

68. Harris JM, Struck EC, Case MG, Paley MS, Vanalstine JM, Brooks DE. Synthesis and characterization of poly(ethylene glycol) derivatives. Journal of Polymer Science Part a-Polymer Chemistry. 1984;22:341-52.

69. Paley MS, Harris JM. Synthesis of the aldehyde of oligomeric polyoxyethylene. Journal of Polymer Science Part a-Polymer Chemistry. 1987;25:2447-54.

70. Lele BS, Kulkarni MG. Single step room temperature oxidation of poly(ethylene glycol) to poly(oxyethylene)-dicarboxylic acid. Journal of Applied Polymer Science. 1998;70:883-90.

71. Lindgren BO, Nilsson T. Preparation of carboxylic-acids from aldehydes (including hydroxylated benzaldehydes) by oxidation with chlorite. Acta Chemica Scandinavica. 1973;27:888-90.

72. Corey EJ, Suggs JW. Pyridinium chlorochromate - Efficient reagent for oxidation of primary and secondary alcohols to carbonyl-compounds. Tetrahedron Letters. 1975:2647-50.

73. Kornblum N, Powers JW. Synthesis of aliphatic nitro compounds. Journal of Organic Chemistry. 1957;22:455-6.

74. Nilsson K, Mosbach K. Immobilization of enzymes and affinity ligands to various hydroxyl group carrying supports using highly reactive sulfonyl chlorides. Biochemical and Biophysical Research Communications. 1981;102:449-57.

75. Nilsson K, Mosbach K. [2] Immobilization of ligands with organic sulfonyl chlorides. In: William BJ, editor. Methods in Enzymology: Academic Press; Oxford; 1984. p. 56-69.

76. Nilsson K, Mosbach K. [3] Tresyl chloride-activated supports for enzyme immobilization. In: Klaus M, editor. Methods in Enzymology: Academic Press; 1987. p. 65-78.

77. Anelli PL, Biffi C, Montanari F, Quici S. Fast and selective oxidation of primary alcohols to aldehydes or to carboxylic-acids and of secondary alcohols to ketones mediated by oxoammonium salts under 2-phase conditions. Journal of Organic Chemistry. 1987;52:2559-62.

78. De Nooy AEJ, Besemer AC, Van Bekkum H. On the use of stable organic nitroxyl radicals for the oxidation of primary and secondary alcohols. Synthesis. 1996:1153-74.

79. Zhao MM, Li J, Mano E, Song ZJ, Tschaen DM. Oxidation of primary alcohols to carboxylic acids with sodium chlorite catalized by TEMPO and bleach: 4-methoxyphenylacetic acid. Organic Syntheses. 2005;81.

80. Bobbitt JM, Flores MCL. Organic nitrosonium salts as oxidants in organic-chemistry. Heterocycles. 1988;27:509-33.

81. Miyazawa T, Endo T, Shiihashi S, Okawara M. Selective oxidation of alcohols by oxoaminium salts (R2n=O+X-). Journal of Organic Chemistry. 1985;50:1332-4.

82. Rychnovsky SD, Vaidyanathan R. TEMPO-catalyzed oxidations of alcohols using m-CPBA: The role of halide ions. Journal of Organic Chemistry. 1999;64:310-2.

83. Dalcanale E, Montanari F. Selective oxidation of aldehydes to carboxylic-acids with sodium-chlorite hydrogen-peroxide. Journal of Organic Chemistry. 1986;51:567-9.

84. Dominguez A, Fernandez A, Gonzalez N, Iglesias E, Montenegro L. Determination of critical micelle concentration of some surfactants by three techniques. Journal of Chemical Education. 1997;74:1227-31.

85. Shedlovsky T. The electrolytic conductivity of some uni-valent electrolytes in water at 25˚C. Journal of the American Chemical Society. 1932;54:1411-28.

86. Kameyama K, Muroya A, Takagi T. Properties of a mixed micellar system of sodium dodecyl sulfate and octylglucoside. Journal of Colloid and Interface Science. 1997;196:48-52.

87. Sarmoria C, Puvvada S, Blankschtein D. Prediction of critical micelle concentrations of nonideal binary surfactant mixtures. Langmuir. 1992;8:2690-7.

88. Holland PM, Rubingh DN. Nonideal multicomponent mixed micelle model. Journal of Physical Chemistry. 1983;87:1984-90.

89. Hua XY, Rosen MJ. Synergism in binary-mixtures of surfactants. 1. Theoretical-analysis. Journal of Colloid and Interface Science. 1982;90:212-9.

90. Detar DF, Silverst.R. Reactions of carbodiimides. I. Mechanisms of reactions of acetic acid with dicyclohexylcarbodiimide. Journal of the American Chemical Society. 1966;88:1013-&.

91. Detar DF, Silverst.R. Reactions of carbodiimides. 2. Reactions of dicyclohexylcarbodiimide with carboxylic acids in presence of amines and phenols. Journal of the American Chemical Society. 1966;88:1020.

92. Rozenman MM, Liu DR. DNA-templated synthesis in organic solvents. Chembiochem. 2006;7:253-6.

93. Staros JV, Wright RW, Swingle DM. Enhancement by N-hydroxysulfosuccinimide of water-soluble carbodiimide-mediated coupling reactions. Analytical Biochemistry. 1986;156:220-2.

94. Grabarek Z, Gergely J. Zero-length crosslinking procedure with the use of active esters. Analytical Biochemistry. 1990;185:131-5.

95. Richert L, Boulmedais F, Lavalle P, Mutterer J, Ferreux E, Decher G, et al. Improvement of stability and cell adhesion properties of polyelectrolyte multilayer films by chemical cross-linking. Biomacromolecules. 2004;5:284-94.

96. Asthagiri AR, Lauffenburger DA. Bioengineering models of cell signaling. Annual Review of Biomedical Engineering. 2000;2:31-53.

97. Horvath G, Lieb T, Conner GE, Salathe M, Wanner A. Steroid sensitivity of norepinephrine uptake by human bronchial arterial and rabbit aortic smooth muscle cells. American Journal of Respiratory Cell and Molecular Biology. 2001;25:500-6.

98. Pozzo-Miller LD, Pivovarova NB, Connor JA, Reese TS, Andrews SB. Correlated measurements of free and total intracellular calcium concentration in

central nervous system neurons. Microscopy Research and Technique. 1999;46:370-9.

99. Sato K, Ozaki H, Karaki H. Differential-effects of carbachol on cytosolic calcium levels in vascular endothelium and smooth-muscle. Journal of Pharmacology and Experimental Therapeutics. 1990;255:114-9.

100. White NS, Errington RJ. Fluorescence techniques for drug delivery research: theory and practice. Advanced Drug Delivery Reviews. 2005;57:17-42.

101. Watson P, Jones AT, Stephens DJ. Intracellular trafficking pathways and drug delivery: fluorescence imaging of living and fixed cells. Advanced Drug Delivery Reviews. 2005;57:43-61.

102. Grynkiewicz G, Poenie M, Tsien RY. A New generation of Ca 2+ indicators with greatly improved fluorescence properties. Journal of Biological Chemistry. 1985;260:3440-50.

103. Napoli A, Valentini M, Tirelli N, Muller M, Hubbell JA. Oxidation-responsive polymeric vesicles. Nature Materials. 2004;3:183-9.

104. Sun HL, Guo BN, Cheng R, Meng FH, Liu HY, Zhong ZY. Biodegradable micelles with sheddable poly(ethylene glycol) shells for triggered intracellular release of doxorubicin. Biomaterials. 2009;30:6358-66.

VITA

Karym Grace Kinnibrugh García received her Bachelor of Science degree in chemistry from the Pontificia Universidad Católica del Perú, Lima, Perú in 2000. She entered the Materials Science and Engineering program at the Pontificia Universidad Católica del Perú, Lima, Perú in 2001 and conducted her Master of Science degree studies until December 2003. She later joined the Materials Science and Engineering program at Texas A&M University in August 2005 and received her Doctor of Philosophy degree in May 2010.

Her research interests include the design, preparation and characterization of functionalized block copolymers vesicles and their application as carrier vehicles for release of drug molecules triggered by their exposure to stimuli responsive environments, as well as the interactions of modified polymer brushes with mammalian cells. Expertise in spectroscopic and microscopy techniques, including: (1) Nuclear Magnetic Resonance (NMR), (2) Fourier-Transform Infrared Spectroscopy (FTIR), (3) UV-Vis Spectroscopy, (4) Fluorescence Spectroscopy, (5) Fluorescence Microscopy, (6) Micropipette Aspiration Technique, (7) Atomic Force Microscopy (AFM), (8) Scanning Electron Microscopy (SEM), (9) Transmission Electron Microscopy (TEM), and, (10) X-Ray Photoelectron Spectroscopy (XPS).

Ms. Kinnibrugh may be reached through Dr. Zhengdong Cheng at the Chemical Engineering Department, Texas A&M University, College Station, TX 77843-3122. Her personal email is karymkh@hotmail.com.